

One-dimensional model of interacting-step fluctuations on vicinal surfaces: Analytical formulas and kinetic Monte-Carlo simulations

Paul N. Patrone^{1,*}, T. L. Einstein^{1,†} and Dionisios Margetis^{2‡}

¹*Department of Physics, University of Maryland, College Park, Maryland 20742, USA*

²*Department of Mathematics, and Institute for Physical Science and Technology,
and Center for Scientific Computation and Mathematical Modeling,
University of Maryland, College Park, Maryland 20742, USA*

(Dated: June 19, 2010)

We study analytically and numerically a one-dimensional model of interacting line defects (steps) fluctuating on a vicinal crystal. Our goal is to formulate and validate analytical techniques for approximately solving systems of coupled, nonlinear stochastic differential equations (SDEs) governing fluctuations in surface motion. In our analytical approach, the starting point is the Burton-Cabrera-Frank (BCF) model, by which step motion is driven by diffusion of adsorbed atoms on terraces and atom attachment-detachment at steps. The step energy accounts for entropic and nearest-neighbor elastic-dipole interactions. By including Gaussian white noise to the equations of motion for terrace widths, we formulate *large systems* of SDEs under different choices of diffusion coefficients for the noise. We simplify this description via (i) perturbation theory and *linearization* of the step interactions and, alternatively, (ii) a *mean-field* (MF) approximation whereby widths of adjacent terraces are replaced by a self-consistent field but nonlinearities in step interactions are retained. We derive simplified formulas for the time-dependent terrace width distribution (TWD) and its steady-state limit. Our MF analytical predictions for the TWD compare favorably with kinetic Monte-Carlo simulations under the addition of a suitably conservative white noise in the BCF equations.

PACS number(s): 81.15.Aa, 05.10.Gg, 68.35.Ja, 05.40.-a

I. INTRODUCTION

Stochastic fluctuations are ubiquitous in material systems. Physical systems of interest that exhibit fluctuations include epitaxially grown crystals [1] as well as biosensors and biologically inspired membranes [2]. The role of stochastic effects in the nonlinear dynamics of crystal surfaces, in particular, has been the subject of extensive studies, both experimental and theoretical [3–7]. In this context, understanding the interplay of nonlinear evolution and noise leads to challenging questions, many of which remain unexplored.

Vicinal crystals are characterized by nanoscale terraces oriented in the high-symmetry direction and separated by line defects (steps) of atomic height [3, 8]. The total number of steps is fixed by the miscut angle of the crystal. The motion of steps drives the dynamics of crystal surfaces at large scales. The step fluctuation laws provide valuable information for the dominant mass transport mechanisms on surfaces of crystalline solids [3].

In this paper, we study by methods of stochastic calculus, asymptotics and kinetic Monte Carlo (kMC) simulations the step fluctuations in a one-dimensional (1D) geometry. The steps are assumed to be straight, monotonic, and interact entropically or as elastic dipoles. This setting leads to a large system of stochastic differential equations (SDEs) for the terrace widths. Our main

goal is to simplify this system and extract explicit formulas for the terrace width distribution (TWD). We invoke two distinct analytical techniques, and compare our results to 1D kMC simulations. Our techniques are: (i) perturbation theory and exact computation of variances for *linearized* SDEs; and (ii) a *mean field* (MF) approximation, on the basis of kinetic Bogoliubov-Born-Green-Kirkwood-Yvon (BBGKY)-type hierarchies [9] for terrace-terrace correlation functions. In the course of our study, we assume that steps interact *strongly* enough in order to enable simplifications.

With this work, we intend to explore advantages and limitations of analytical techniques, e.g., the MF approach, for large stochastic systems in a relatively simple setting (which allows tractable yet nontrivial computations). Our approach aims to complement previous treatments of step fluctuations in the presence of material deposition from above in 1D [7, 10]. In [7, 10], steps are non-interacting and the related SDEs are perturbed around the terrace width average. In the present paper, we introduce the more realistic element of *dipolar step-step interactions* and retain nonlinearities in the SDEs. As a result, a noncrossing condition for steps is drastically enforced. In the MF picture, the germane SDEs lead to a nonlinear equation for the stochastic process of a single terrace. The corresponding Fokker-Planck-type equation (FPE) unravels a rich behavior of the TWD. In principle, linearized models fail to capture essential features of this behavior. Our approach points to this conclusion via MF approximations consistent with BBGKY hierarchies, and comparisons with kMC simulations.

Our analysis is mainly limited by (i) the 1D character of the geometry, and (ii) our assumption of statistical

*ppatrone@umd.edu

†einstein@umd.edu

‡dio@math.umd.edu

independence in implementing the MF approximation. First, the steps are straight and, thus, their meandering and curvature are eliminated. This simplification yields, as an artifact, a singularity of the TWD at zero terrace width, which mathematically enforces a step noncrossing condition. Second, to allow for tractable computations in the MF picture, we assume that the terrace widths are decorrelated, so that their joint probability distributions, $p^{(n)}$, are approximated by products of TWDs. We claim that, despite the above limitations, some elements of our techniques, e.g., the self-consistent generation of a mean field for terraces from kinetic hierarchies, can be extended to two-dimensional (2D) settings.

The model of step flow originates from the pioneering work by Burton, Cabrera, and Frank (BCF) [11]. In the BCF model, the motion of steps is caused by mass conservation as adsorbed atoms (adatoms) diffuse across terraces and detach from or attach to step edges. A key assumption is that adatoms are represented by a concentration that satisfies a diffusion equation on each terrace. The laws for atom attachment-detachment are introduced as boundary conditions [3, 11]. In the original BCF model [11], steps are non-interacting, but later works enrich this theory with entropic and elastic-dipole step interactions [12–14]. A crucial thermodynamic quantity relating motion with energy is the step chemical potential [3], which expresses the tendency of a step to advance or retreat via exchanging atoms with the environment.

By adding Gaussian white noise to the BCF-type step equations, we formulate a system of SDEs for terrace widths. These SDEs have the form

$$\dot{\mathbf{w}}(t) = \mathbf{a}(\mathbf{w}) + \mathbf{Q} \cdot \dot{\boldsymbol{\eta}}(t) , \quad (1)$$

where $\mathbf{w} = (w_0, \dots, w_{N-1})$ is the vector of N terrace widths; \mathbf{a} is another N -dimensional vector encapsulating step-step interactions and in principle depending on \mathbf{w} non-linearly; \mathbf{Q} is the $N \times N$ diffusion coefficient; and $\dot{\boldsymbol{\eta}}$ is the vector-valued Gaussian white noise, i.e, the derivative (in the sense of distributions) of the Brownian motion $\boldsymbol{\eta} = (\eta_0, \dots, \eta_{N-1})$ [15]. The dot on top of a symbol denotes differentiation in time, t , throughout. We apply screw-periodic boundary conditions for w_j and η_j , so that the steps are mapped onto point particles on a ring.

In Eq. (1), $\mathbf{Q} \cdot \dot{\boldsymbol{\eta}}$ is intended to model effects of random thermal fluctuations and couplings with the environment. This *ad hoc* approach, where the noise form is assumed rather than derived by first principles, has been motivated by [7, 10]. To allow for some flexibility in modeling, we consider three forms of \mathbf{Q} amounting to: (i) $(\mathbf{Q} \cdot \boldsymbol{\eta})_j = \dot{\eta}_j(t)$, i.e., the usual non-conservative white noise; (ii) $(\mathbf{Q} \cdot \boldsymbol{\eta})_j = \dot{\eta}_{j+1} - \dot{\eta}_j$, a first-order conservative scheme; and (iii) $(\mathbf{Q} \cdot \boldsymbol{\eta})_j = \dot{\eta}_{j+1} - 2\dot{\eta}_j + \dot{\eta}_{j-1}$, a second-order conservative scheme. We show that only choice (iii) is compatible with the requirements of fixed system size and finite variance. Solving Eqs. (1) poses a challenge. Our primary task here is to reduce the large system of coupled SDEs, Eq. (1), to a tractable FPE and solve for the time-dependent TWD.

We derive asymptotic formulas for the TWD, assuming step interactions are sufficiently large. The difficulty of the large system dimension is addressed in two alternate ways. First, we consider the exactly solvable case of linearizing $\mathbf{a}(\mathbf{w})$ around $\mathbb{E}\mathbf{w} \equiv \langle \mathbf{w} \rangle$, the expectation of \mathbf{w} , i.e., the average terrace width. Our ensuing solution for the stochastic process of terrace widths manifests the interplay between interactions and noise, and sheds some light on effects of step correlations. The results for the terrace width variance under linearization motivate our second, alternate approach: a MF formalism, by which, in the j th SDE, the terms $w_{j\pm 1}$ and $w_{j\pm 2}$ are replaced by an effective field depending on w_j (and time, t). This approximation, partly analyzed via BBGKY hierarchies here and in [10], refines our analysis since it retains nonlinearities.

At the risk of redundancy, we emphasize that a limitation of our theory stems from the 1D character of the underlying model. Thus, step edge diffusion and step meandering are not addressed here. This simplification impedes direct comparisons with experiments. However, our 1D model enables us to: (i) formulate analytically tractable SDEs for *many* terrace widths; and (ii) connect explicitly (via asymptotics) properties of coefficients in these SDEs, e.g., the dipolar form of step interactions, to the global behavior of the TWD. Thus, in this framework, valuable information for the TWD is singled out with reasonable ease. In a 2D setting, on the other hand, complications arise due to step curvature, as well as richer kinetics and forms of noise [4, 5, 16]. This direction is left for near-future work.

Another limitation is the MF approximation, which we do not justify rigorously. This scheme has been used in previous studies of step dynamics [6, 7]. By invoking BBGKY hierarchies for joint probability density functions of terrace widths, we define the MF exactly, and then simplify the SDEs on the basis of a statistical independence (“propagation of chaos”) hypothesis, in the spirit of Ref. [10]. This hypothesis is not strictly satisfied in step systems but, via comparisons with the linearized model, is expected to be a reasonable approximation for short or long enough times (for a class of initial data) [10]. Interestingly, we find agreement of our MF solution with the 1D kMC simulations for moderate to strong step interactions.

An ultimate justification for the analytic manipulations in our work relies on the use of kMC simulations in 1D. Broadly speaking, the kMC approach has been used extensively in the study of surfaces in 2D; e.g., see [7]. In some instances, physical effects such as entropic repulsion are inherent to the kMC algorithms.

Since we carry out kMC simulations for 1D step trains, the details of implementing our numerical approach are strictly different from corresponding simulations in 2D. An element of our algorithm is to assign to each step (“particle”), a probability of movement to another 1D site; this probability depends on the energy barrier that the step must overcome. Each particle is coupled to two

nearest neighbors on each side, where the particle interaction is an inverse-distance squared potential. The algorithm is based on a scheme described in Ref. [17].

The remainder of the paper is organized as follows: Section II introduces our model and the governing SDEs for terraces. Section III describes the linearization of these SDEs and the extraction of the terrace width variance in the limit as $N \rightarrow \infty$ for finite times. Notably, our main result contains analytical features, e.g., scaling of time scale with step interaction strength, that persist in the nonlinear case. Section IV focuses on the MF formalism via the notion of kinetic hierarchy. In Sec. V, we develop a MF approximation scheme for computing the steady-state TWD for a sufficiently large interaction parameter. This scheme is motivated by the observation that, for nonlinear SDEs, the (self-consistent) mean field in principle does *not* coincide with the average terrace width. Section VI focuses on an extension of this approximation to the time-dependent TWD. In Sec. VII, we discuss extensions and limitations of our treatment. Finally, Sec. VIII summarizes our results.

Notation and terminology. Throughout the paper, we adhere to certain notation conventions. Vectors are lowercase and matrices uppercase; both objects are boldface unless we indicate otherwise. For any *circulant* matrix $\mathbf{\Lambda}$, the (nonnegative) quantity $|\mathbf{\Lambda}|^2$ is the sum of the magnitudes squared of elements of the first row of $\mathbf{\Lambda}$. We adopt the Einstein summation convention, i.e., we sum over repeated indices. The symbol \mathbb{R}_n^+ denotes the region of the n -dimensional Euclidean space (\mathbb{R}_n) with nonnegative coordinates. The symbol ∂_z denotes partial differentiation with respect to z (i.e., $\partial_z \equiv \partial/\partial z$). By writing $f = \mathcal{O}(g)$ ($f = o(g)$) we imply that f/g is bounded by a constant ($f/g \rightarrow 0$) as a parameter or variable approaches an extreme value. Accordingly, the expression $f \sim g$ loosely implies $f - g = o(g)$. The probabilistic terms “average” and “expectation” are used interchangeably. Further, we do *not* distinguish the terms “distribution” and “probability density”. We reserve the symbol $P(s, t)$ for the TWD, and $p^{(n)}(s, t)$ for the joint probability density of any n consecutive terraces (if $n \geq 2$).

II. BACKGROUND: BCF MODEL

In this section, we review the physical principles underlying our model, which are based on the kinetic perspective of BCF [11]. This perspective has been enriched with kinetic and energetic effects; see, e.g., Refs. [18–23]. The main idea is to view steps as boundaries moving by mass conservation. Adatoms diffuse on terraces between steps according to a (continuum) differential equation. In addition, atoms attach to and detach from step edges with given kinetic rates. The interactions between steps are included in the boundary (attachment-detachment) conditions for adatom diffusion. These interactions influence the flux of adatoms towards step edges via the step chemical potential, a thermodynamic force.

We start by considering a 1D train of N steps which have (constant) height a and are descending in the positive x direction (see Fig. 1). For simplicity of notation, we take the lattice to be simple cubic, with terraces in an $\{001\}$ direction, so that the in-plane square lattice also has lattice constant a . Let the step positions be labeled by an (integer) index, j , where $j = 0, 1, \dots, N - 1$. Define the j th terrace width by $w_j = x_j - x_{j-1}$. We apply screw periodic boundary conditions, so that the steps are mapped onto particles on a ring [7, 10].

Let \tilde{t} be the physical (dimensional) time. The number density, $c_j(x, \tilde{t})$, of adatoms on the j th terrace solves the equation [11]

$$D\partial_{xx}c_j(x, \tilde{t}) = \partial_{\tilde{t}}c_j(x, \tilde{t}) \quad \text{for } x_{j-1} < x < x_j, \quad (2)$$

subject to the boundary conditions [3, 20, 24]

$$\begin{aligned} \mathcal{J}_j^- &= k_-[c_j(x_j) - c_j^{\text{eq}}], \\ \mathcal{J}_{j-1}^+ &= k_+[c_j(x_{j-1}) - c_{j-1}^{\text{eq}}]. \end{aligned} \quad (3)$$

In the above, D is the terrace diffusivity and \mathcal{J}_j^\pm is the mass flux impinging on the j th step from right (+) or left (−) with kinetic rates k_\pm [25, 26]. The quantity c_j^{eq} is the equilibrium adatom concentration at the j th step edge, and is given by the near-equilibrium relation [3]

$$c_j^{\text{eq}} = c_s \exp\left(\frac{\mu_j}{k_B T}\right) \simeq c_s \left(1 + \frac{\mu_j}{k_B T}\right), \quad (4)$$

if $|\mu_j| \ll k_B T$. Note that μ_j is the j th-step chemical potential, c_s is a material-dependent constant, and $k_B T$ is the Boltzmann energy. For entropic and elastic-dipole step interactions, μ_j is expressed as [3]

$$\mu_j = \tilde{g}a^3 \left(\frac{1}{w_{j+1}^3} - \frac{1}{w_j^3}\right), \quad \tilde{g} > 0, \quad (5)$$

where the coupling constant \tilde{g} has units of energy.

To solve Eq. (2), we adopt the *quasi-static approximation*, by which each $c_j(x, \tilde{t})$ is assumed to reach its steady state much faster than steps move. Hence, set $\partial_{\tilde{t}}c_j(x, \tilde{t}) \equiv 0$ for every j . Accordingly, the adatom flux on the j th terrace, $J_j(x, \tilde{t}) = -D\partial_x c_j(x, \tilde{t})$, is a constant,

$$J_j(x) = D \frac{c_{j-1}^{\text{eq}} - c_j^{\text{eq}}}{\frac{D}{k_-} + \frac{D}{k_+} + w_j} \quad \text{for } x_{j-1} < x < x_j. \quad (6)$$

By Eq. (3), in the quasi-static approach we use $\mathcal{J}_{j-1}^+ = -J_j(x_{j-1})$ and $\mathcal{J}_j^- = J_j(x_j)$ since any convective contributions to \mathcal{J} due to the step velocity are negligible.

By mass conservation, the j -th step velocity is [3, 11]

$$\dot{x}_j(\tilde{t}) = \frac{dx_j}{d\tilde{t}} = \frac{\Omega}{a}(J_j - J_{j+1}) = a(J_j - J_{j+1}), \quad (7)$$

where $\Omega = a^2$ is the surface atomic area. Equation (7), combined with Eqs. (4)–(6), leads to the following (deterministic) equations of motion for terrace widths:

$$\begin{aligned} \dot{w}_j &= \dot{x}_j - \dot{x}_{j-1} \\ &= 2\tilde{g}H(w_j; w_{j-1}, w_{j+1}) - \tilde{g}H(w_{j+1}; w_j, w_{j+2}) \\ &\quad - \tilde{g}H(w_{j-1}; w_{j-2}, w_j), \end{aligned} \quad (8)$$

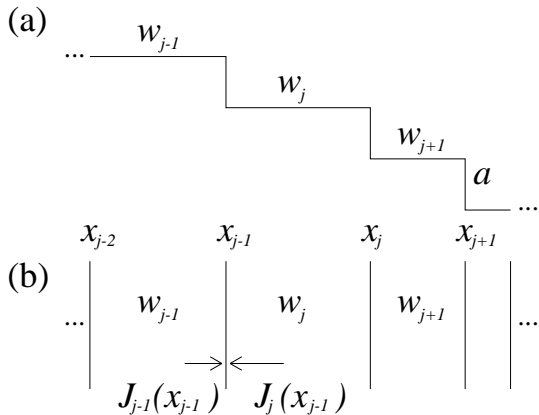


FIG. 1. Side and top views of step system. Steps have height a and positions x_j , and $w_j = x_j - x_{j-1}$. (a) Side view: Steps descend for increasing x . (b) Top view: The directions and magnitudes of adatom fluxes $J_{j-1}(x)$ and $J_j(x)$ at $x = x_{j-1}$ are represented by arrows; by Eq. (7), the $(j-1)$ th step edge moves to the right.

where

$$H(x; y, z) = \frac{1}{\check{c} + x} \left[\frac{2}{x^3} - \left(\frac{1}{y^3} + \frac{1}{z^3} \right) \right]. \quad (9)$$

For a vicinal surface, we take the initial condition $w_j(0) = \langle w \rangle$ (although in principle we could start more generally with N constants with average value $\langle w \rangle$). Here, the parameter $\check{g} = Dc_s \tilde{g} a^4 / k_B T$ is a measure of the interaction strength, and $\check{c} = D(k_+^{-1} + k_-^{-1})$ is a kinetic length expressing the interplay of diffusion and attachment-detachment processes. We make Eq. (8) dimensionless by setting $s_j = w_j / \langle w \rangle$ and $t = \tilde{t} / t^*$ where t^* is some time scale, e.g., $t^* = \langle w \rangle^2 / D$. We also define $g = \check{g} t^* / \langle w \rangle^5$ and $c = \check{c} / \langle w \rangle$. We have $\langle s_j \rangle = 1$, which fixes the vicinal crystal size.

To model fluctuations, we add a term containing a Gaussian white noise to Eq. (8). Since our approach is ad hoc (i.e., the noise form is assumed and not derived from first principles), we allow for some flexibility in the choice of the noise term. We write

$$\dot{s}_j = \frac{ds_j}{dt} = gA(s_{j-2}, s_{j-1}, s_j, s_{j+1}, s_{j+2}) + Q_{j,l} \dot{\eta}_l, \quad (10)$$

where $\dot{\eta}_l$ ($l = 0, \dots, N-1$) is the Gaussian white noise at the l th step, and $\mathbf{Q} = [Q_{j,l}]$ is some $N \times N$ matrix (to be specified below). Note that before non-dimensionalizing, the coefficient multiplying $\dot{\eta}_l$ is $(D/\langle w \rangle)Q_{j,l}$, which has units length over time. We also define

$$\begin{aligned} A(s_{j-2}, s_{j-1}, s_j, s_{j+1}, s_{j+2}) &= 2H(s_j; s_{j-1}, s_{j+1}) \\ &- H(s_{j-1}; s_{j-2}, s_j) - H(s_{j+1}; s_j, s_{j+2}), \end{aligned} \quad (11)$$

i.e., the right-hand side of Eq. (8) divided by g , where \check{c} is now replaced by c in H (see Eq. (9)). Note that in Eq. (10) we single out the constant g . This g influences the time and length scales for the dynamical system. In Secs. V and VI, we show analytically how the singular character of A prohibits step crossing.

Equation (10) is the main result of this section and forms the basis of our subsequent calculations. In Secs. III–VI, we develop techniques for extracting statistical properties of the terrace widths by further analyzing Eq. (10) via stochastic calculus and kinetic hierarchies.

The above model has limitations. First, steps are straight; hence, the effects of curvature and step meandering [4, 5] are omitted from our formulation. Despite this restriction due to dimensionality, the deterministic system (8) has been used in the study of relaxation of step bunches in certain material systems; see, e.g., [20]. Second, material deposition, which is included in other stochastic treatments [7, 10], is not present in our model. The combined effect of deposition, step-step interactions and noise is left for near-future work.

III. LINEARIZED MODEL

In this section, we aim to gain some insight into the stochastic fluctuations and correlations of terrace widths via the linearization and exact solution of Eq. (10). In our manipulations, we consider the limit as $N \rightarrow \infty$ for fixed (N -independent) time, t , in the spirit of [10]. The quantity of interest is the terrace width *variance* as a function of time. We discuss the effect on the variance of different choices for the diffusion coefficient, \mathbf{Q} . In particular, we choose the simplest possible (yet nontrivial) \mathbf{Q} for which the variance is consistent with a fixed system size and settles to a finite limit at the steady state.

The linearization of this section results in an unphysical property: the probability that terrace widths are negative (and, thus, steps cross) is nonzero [7, 10]. We adopt the view that this probability can be controlled: it becomes small if the step-step interaction strength (g) is sufficiently large [27]. We focus on the TWD $P(s)$, bearing in mind that our result should be accurate for s close enough to the TWD peak. This knowledge partly motivates and guides our analysis in the nonlinear case if $g \gg 1$, when step fluctuations are reasonably small.

Hence, proceeding under the assumption that $g \gg 1$, we treat the stochastic fluctuation process $\varpi_j = s_j - 1$ as small in the sense that $1 - \text{Prob}\{|\varpi_j| < \epsilon\} \ll 1$ for sufficiently small $\epsilon > 0$ (where the Prob denotes the probability). It is then reasonable to expand the governing Eqs. (10) around $\varpi_j = 0$ ($j = 0, \dots, N-1$). Defining $g_c = 3g/(c+1)$, we derive the linear SDE system

$$\begin{aligned} \dot{\varpi}_j(x) &= -g_c[6\varpi_j - 4(\varpi_{j-1} + \varpi_{j+1}) \\ &+ \varpi_{j-2} + \varpi_{j+2}] + Q_{j,l} \dot{\eta}_l, \end{aligned} \quad (12)$$

where (abusing notation) we keep the same symbol, ϖ_j , for the approximate solution. In contrast to Refs. [7, 10]

where the discrete scheme is of second order, SDEs (12) introduce *fourth-order* couplings. Note in passing that in the continuum limit, Eq. (12) reduces to a fourth-order differential equation.

Now let ϖ and η be vectors whose components are the fluctuations and noise, respectively, of each terrace; e.g., $\varpi = (\varpi_0, \dots, \varpi_{N-1})$. Define \mathbf{A} to be the circulant matrix whose first row is $[6, -4, 1, 0, \dots, 0, 1, -4]$. Equation (12) is then written more compactly as

$$\dot{\varpi} = -g_c \mathbf{A} \cdot \varpi + \mathbf{Q} \cdot \dot{\eta}. \quad (13)$$

By enforcing the initial condition $\varpi(0) = 0$, we trivially solve Eq. (13) by means of an integrating factor:

$$\varpi(t) = \int_0^t e^{-g_c \mathbf{A}(t-t')} \mathbf{Q} \cdot d\eta(t'), \quad (14)$$

without any ambiguity in interpreting the stochastic integral. The stochastic process $\varpi(t)$, as well as each of its components, is Gaussian with zero mean [15]. The variance for any terrace width, ϖ_j , at time t is

$$\sigma_{\text{lin}}^2(t) = g_c^{-1} \int_0^{g_c t} |e^{-\tau' \mathbf{A}} \mathbf{Q}|^2 d\tau'. \quad (15)$$

To compute $\sigma_{\text{lin}}^2(t)$ by Eq. (15), we use a spectral property of circulant matrices. Specifically, for any real circulant $N \times N$ matrices \mathbf{X} and \mathbf{Y} , we have (see Appendix A)

$$|\mathbf{X} e^{\mathbf{Y}}|^2 = \frac{1}{N} \sum_{k=0}^{N-1} \vartheta_k e^{\lambda_k}, \quad (16)$$

where λ_k are the eigenvalues of the matrix $\mathbf{Y} + \mathbf{Y}^T$ and ϑ_k are the eigenvalues of $\mathbf{X} \mathbf{X}^T$. Furthermore, note that the k th eigenvalue of any circulant $N \times N$ matrix \mathbf{A} is furnished by the product $F_{k,l} \Lambda_{l,0}$, where \mathbf{F} is the $N \times N$ discrete Fourier transform matrix, $F_{k,l} = [\mathbf{F}]_{k,l} = e^{-2\pi i(kl)/N}$. In the following, we use Eq. (16) for the evaluation of σ_{lin}^2 by Eq. (15).

A. First-order conservative noise

At this point, it is necessary to make a specific choice for \mathbf{Q} . We require that the total size of the vicinal crystal be fixed. This implies that summing Eqs. (12) over all j should lead to a deterministic evolution equation. Accordingly, the sum of elements in any row (or column) of \mathbf{Q} must be zero. If, instead, this condition is violated, e.g., when $\mathbf{Q} = \mathbf{1}$ (identity matrix), summing Eqs. (12) over all j yields an SDE for the total fluctuations of the system that is solved by a Brownian-motion-like stochastic process (with a nonzero variance growing with time).

An apparently reasonable choice for \mathbf{Q} , consistent with the requirement of fixed system size, can stem from setting its first row equal to $[1, -1, 0, 0, \dots]$. This matrix

corresponds to a *first-order*, conservative discrete scheme for the noise term. This model of noise simply results by addition of the usual white noise component, $\dot{\eta}_j$, to each *step velocity*, \dot{x}_j . Nonetheless, in Appendix B we show that the corresponding variance *diverges* for long times; specifically, we find $\sigma_{\text{lin}}^2(t) = \mathcal{O}[(g_c t)^{1/4}]$ as $t \rightarrow \infty$. Thus, we abandon this option as well.

B. Second-order conservative noise

The next simplest (yet nontrivial) choice for \mathbf{Q} amounts to a *second-order* scheme for a conservative noise. Accordingly, we set the first row of \mathbf{Q} equal to $[2, -1, 0, \dots, 0, -1]$. This choice is consistent with the above requirements: a fixed total system size and bounded TWD variance [28]. The self-consistent form of \mathbf{Q} is not unique; by speculation, we make the simplest choice that works. This approach does not weaken the argument for linearizing the model and yields insight into the interplay of noise and step kinetics. In Secs. IV–VI, where we consider an effective MF Langevin-type equation for a single terrace, we show that the \mathbf{Q} contributes a constant prefactor to the noise term of the decoupled SDE.

With this choice of \mathbf{Q} in Eq. (15), we find by Eq. (16) that the variance is

$$\sigma_{\text{lin}}^2(t) = g_c^{-1} \int_0^{g_c t} \frac{4}{N} \sum_{k=0}^{N-1} \left\{ \left[1 - \cos\left(\frac{2\pi k}{N}\right) \right]^2 \times e^{-4\tau' [3 - 4 \cos(\frac{2\pi k}{N}) + \cos(\frac{4\pi k}{N})]} d\tau' \right\}. \quad (17)$$

In the limit $N \rightarrow \infty$ with fixed t , the discrete variable k/N approaches a continuous variable, say y ($0 < y < 1$). Thus, Eq. (17) becomes

$$\sigma_{\text{lin}}^2(t) = 4g_c^{-1} \int_0^{g_c t} \int_0^1 [1 - \cos(2\pi y)]^2 \times e^{-8\tau' [1 - \cos(2\pi y)]^2} dy d\tau'. \quad (18)$$

This formula is simplified by interchange of the order of integration:

$$\sigma_{\text{lin}}^2(t) = \frac{1}{2g_c} \left[1 - \int_0^1 e^{-8g_c t [1 - \cos(2\pi y)]^2} dy \right], \quad (19)$$

the variance of approximation LM in figures. In Appendix B, we compute integral (19) exactly in terms of a series involving modified Bessel functions, but the resulting formula is useful only for small $g_c t$. We show that $\sigma_{\text{lin}}^2(t) = (2g_c)^{-1} [1 + \mathcal{O}[(g_c t)^{-1/4}]]$ as $g_c t \rightarrow \infty$.

Salient features of the variance can be deduced by inspection of Eq. (19), without further evaluation. We observe that the parameter g_c scales both the variance and its time decay to steady state. We expect that the nonlinear model exhibits similar behavior when g_c is large, since stochastic fluctuations are then suppressed and the major contribution to moments of $P(s)$ comes from s

near the location of its peak, away from $s = 0$. Clearly, the linearized model fails to describe $P(s)$ for small s , because this model violates the step noncrossing condition.

For completeness, we conclude this section with the formula for the time-dependent TWD under linearization [15]:

$$P_{\text{lin}}(s, t) = \sqrt{\frac{1}{2\pi\sigma_{\text{lin}}^2(t)}} \exp\left[-\frac{(s-1)^2}{2\sigma_{\text{lin}}^2(t)}\right]. \quad (20)$$

The symmetry of this TWD around $s = 1$ reflects the failure of the linearized model to enforce step noncrossing. However, the probability of having negative terrace widths is negligible provided $g_c \gg 1$. In the remainder of this paper, we use the \mathbf{Q} discussed in this subsection.

IV. MEAN-FIELD FORMALISM

In this section, we introduce a systematic procedure to decouple SDEs (10), i.e., reduce them to a single nonlinear SDE, taking into account the full nonlinearity of the step interactions. This approach aims to complement and improve the linearization procedure of Sec. III. Our scheme relies on the use of an effective mean field, f , which in principle depends on the dimensionless terrace-width variable, s , and time. In principle, f is *not* the average terrace width. The starting point is to consider each of Eqs. (10), for fixed j , and replace $s_{j\pm 1}$ and $s_{j\pm 2}$ by $f(s_j, t)$ [6, 7, 10]. The field f is *not* known a priori but must be determined consistently with the assumption that the resulting SDEs generate a TWD sufficiently close to the TWD of the original system [10].

Thus, in brief our goals for this section are: (i) to find heuristically the FPE for the MF TWD (Sec. IV A); (ii) to derive an exact evolution equation for the TWD in terms of joint probability densities (Sec. IV B); and (iii) to determine by self-consistency an equation for the mean field $f(s, t)$ (Sec. IV C). In Secs. V and VI, this MF formalism is used to describe analytically the TWD in the steady-state and time-dependent cases under the hypothesis of statistical independence for terrace widths.

A. Effective mean-field equations

Now consider Eq. (10) for fixed j . By the above prescription [6, 7, 10], i.e., replacement of $s_{j\pm 1}$ and $s_{j\pm 2}$ by $f(s_j, t)$ for each j , we obtain the effective SDE

$$\frac{d\hat{s}_j}{dt} = gA(\hat{s}_j, f) + \hat{q}\dot{\eta}, \quad (21)$$

where the hat indicates the MF approximation and $A(s, f)$ is used in place of $A(f, f, s, f, f)$:

$$A(s, f) \equiv A(f(s, t), f(s, t), s, f(s, t), f(s, t));$$

see definition (11). Note the coefficient \hat{q} in Eq. (21): this \hat{q} is a number, within the MF approximation, that comes from the matrix \mathbf{Q} via treatment of the noise components $\dot{\eta}_j$ as statistically independent of each other. For \mathbf{Q} with first row equal to $[2, -1, 0, \dots, 0, -1]$ (second-order conservative scheme), we will determine that $\hat{q}^2 = 6$ (see Sec. IV C).

We point out that the existence of a field $f(s, t)$ consistent with the original SDEs (10) is not guaranteed. Our justification for adopting this procedure rests with our comparisons with numerical kMC results. We emphasize that the self-consistency means that the MF approximation produces essentially the time-dependent TWD of system (10) [10]. We elaborate on this idea in Sec. IV C. For the time being, we distinguish the MF TWD from the (exact) $P(s, t)$.

Equation (21) yields a corresponding FPE for the MF TWD, $\hat{P}(s, t)$ [29]:

$$\partial_t \hat{P} + g\partial_s[A(s, f)\hat{P}(s, t)] = \frac{\hat{q}^2}{2}\partial_{ss}\hat{P}(s, t), \quad (22)$$

with the initial and boundary conditions

$$\hat{P}(s, 0) = \delta(s-1), \quad (23a)$$

$$\frac{\hat{q}^2}{2}\partial_s \hat{P} - gA(s, f)\hat{P} \rightarrow 0 \quad \text{as } s \rightarrow 0^+, \infty. \quad (23b)$$

The initial condition (23a) describes a vicinal crystal: the surface slope is constant and all terraces have the same width (scaled to unity). In words, boundary conditions (23b) state that the *probability flux* must vanish as $s \rightarrow 0$ from above and $s \rightarrow \infty$. Thus, steps are prohibited from crossing or moving infinitely far apart. We emphasize that nonlinear SDE (21) does allow for the vanishing of the probability flux at $s = 0$ nontrivially, in contrast to the linearized model of Sec. III.

In Refs. [6, 7, 10], MF descriptions for 1D step models are derived under the assumption that $f(s, t)$ is equal to the average terrace width for all times $t > 0$. In Ref. [10], this assumption is shown to be self consistent only for the case of linear SDEs. In the present case we do not expect the mean field f to coincide with the average terrace width, and the determination of f constitutes a complicated problem. The argument that views f as an average of the stochastic process (terrace width) foreshadows the true role of f , namely, to reconcile the asymmetries introduced by the nonlinear step-step interactions with the requirement of fixed system size. In Sec. V we show how corrections for f in the steady state shift the peak of the TWD to the left of $s = 1$ (average), in agreement with kMC simulations.

B. Evolution law for TWD via kinetic hierarchy

In this subsection, we derive an evolution equation for the exact TWD, $P(s, t)$, on the basis of a kinetic hierarchy for joint probability densities of consecutive ter-

paces. This equation serves our purpose of defining a self-consistent $f(s, t)$ (Sec. IV C).

Following the formalism of Ref. [10], we define the N -terrace distribution $p^{(N)}(\mathbf{s}, t)$, where $\mathbf{s} = (s_0, s_1, \dots, s_{N-1})$; hence, $p^{(N)}(\mathbf{s}, t) d\mathbf{s}$ is the probability that N terraces have widths with values in the intervals $(s_k, s_k + ds_k)$ where $k = 0, \dots, N-1$ and $d\mathbf{s} = ds_0 \cdots ds_{N-1}$. The probability density for *any* n consecutive terraces ($n = \mathcal{O}(1) \geq 2$) is defined by

$$p^{(n)}(\mathbf{s}_{(n)}) = \frac{1}{N} \sum_{k=0}^{N-1} \int_{\mathbb{R}_{N-n}^+} d\mathbf{s}_{(N-n)} p^{(N)}(\mathbf{s}_{(n)}, \mathbf{s}_{(N-n)})_k^c, \quad (24)$$

where $\mathbf{s}_{(n)} = (s_0, \dots, s_{n-1})$, $\mathbf{s}_{(N-n)} = (s_n, \dots, s_{N-1})$, and \mathbf{z}_k^c denotes the vector formed after k cyclic permutations of coordinates of $\mathbf{z} = (\mathbf{s}_{(n)}, \mathbf{s}_{(N-n)})$. In the above, we suppress the time dependence. The desired TWD is

$$P(s, t) = \frac{1}{N} \sum_{k=0}^{N-1} \int_{\mathbb{R}_{N-1}^+} d\mathbf{s}_{(N-1)} p^{(N)}((s, \mathbf{s}_{(N-1)})_k^c, t). \quad (25)$$

Using Eq. (10) we write down the (N -dimensional) FPE for the N -terrace probability density [15, 29]:

$$g \partial_{s_l} [A(s_{l-2}, s_{l-1}, s_l, s_{l+1}, s_{l+2}) p^{(N)}(\mathbf{s}, t)] \\ = -\partial_t p^{(N)}(\mathbf{s}, t) + \frac{1}{2} \partial_{s_l} \partial_{s_k} [\mathbf{Q}^2]_{l,k} p^{(N)}(\mathbf{s}, t), \quad (26)$$

where $A(s_{l-2}, s_{l-1}, s_l, s_{l+1}, s_{l+2})$ is defined by Eq. (11) and $\mathbf{Q} = \mathbf{Q}^T$ is the circulant matrix whose first row is $[2, -1, 0, \dots, 0, -1]$. Recall that we pick this \mathbf{Q} since the TWD must approach a steady state (see Eq. (19)).

To find an evolution equation for $P(s, t)$, apply ∂_t to Eq. (25) and use Eq. (26). Thus, P satisfies [10]

$$\partial_t P(s, t) = -g \partial_s \int_{\mathbb{R}_+^+} \mathcal{A}(s, \vec{y}) p^{(5)}(s, \vec{y}, t) d\vec{y} + 3 \partial_{ss} P(s, t), \quad (27)$$

where for notational economy we use $\mathcal{A}(s, \vec{y})$ in place of $A(y_{N-2}, y_{N-1}, s, y_1, y_2)$ and we employ $p^{(5)}(s, \vec{y})$ to mean $p^{(5)}(y_{N-2}, y_{N-1}, s, y_1, y_2)$; $\vec{y} = (y_{N-2}, y_{N-1}, y_1, y_2)$ and $d\vec{y} = dy_{N-2} dy_{N-1} dy_1 dy_2$. Equation (27) suffices for defining the mean field, f . Evolution equations for $p^{(n)}$ ($n \geq 2$) can be written in a similar fashion, but lie beyond our scope.

C. Definition of mean field f

In this subsection, we combine Eqs. (22) and (27) in order to extract a formula for the mean field, $f(s, t)$. Thus, we assume there exists an f such that [10]

$$\hat{P}(s, t) \equiv P(s, t). \quad (28)$$

This equation expresses the hypothesis that the exact TWD, $P(s, t)$, coincides with the MF TWD. We choose

$\hat{q} = \sqrt{6}$ since then subtracting Eq. (27) from Eq. (22) yields

$$A(s, f(s, t)) P(s, t) = \int_{\mathbb{R}_+^+} \mathcal{A}(s, \vec{y}) p^{(5)}(s, \vec{y}, t) d\vec{y}. \quad (29)$$

This is the desired formula for $f(s, t)$. It simply states that in order to compute f one must in principle know the 5-terrace joint probability density. Equation (29) may be simplified via the 3-terrace probability density, $p^{(3)}$, by taking into account the particular form of A , Eq. (11):

$$A(s, f(s, t)) P(s, t) = \\ 2 \int_{\mathbb{R}_2^+} H(s; y_2, y_1) p^{(3)}(y_2, s, y_1, t) dy_1 dy_2 \\ - \int_{\mathbb{R}_2^+} H(y_2; y_1, s) p^{(3)}(y_1, y_2, s, t) dy_1 dy_2 \\ - \int_{\mathbb{R}_2^+} H(y_1; s, y_2) p^{(3)}(s, y_1, y_2, t) dy_1 dy_2. \quad (30)$$

In the remainder of this paper, we apply a hypothesis of statistical independence for terraces (if $N \gg 1$) which simplifies Eq. (30) by reducing its right-hand side to integrals involving the product $P(y_1)P(y_2)$.

V. STEADY-STATE MEAN FIELD

In this section, we develop an approximation scheme in order to find the TWD in the steady state, i.e., when $\partial_t P(s, t) \equiv 0$. The primary task is to propose a *closure* for and then solve Eqs. (22) and (30) for the TWD P and mean field f . These equations must in principle be complemented with the entire BBGKY hierarchy. We avoid the complication of the kinetic hierarchy by applying approximations, which come from: (i) a decorrelation hypothesis for terraces, so that the $p^{(3)}$ in Eq. (30) is written as $p^{(3)}(y_2, s, y_1) \approx P(y_2)P(s)P(y_1)$, which automatically implies invariance of $p^{(3)}$ under permutations of its arguments (s, y_1 and y_2); and (ii) subsequent expansions of $f(s)$ and $P(s)$ in power series in the interaction strength g for $g \gg 1$. We compare our analytical results for the steady-state TWD with kMC simulations. Details of our 1D kMC algorithm (also invoked in Sec. VI) are provided in Appendix C.

A. Formulation

We start with a remark on Eq. (30). If we naively set $p^{(3)}(s, y_1, y_2) = \delta(s-1)\delta(y_1-1)\delta(y_2-1)$ and $P(s) = \delta(s-1)$, Eq. (30) is satisfied trivially by $f = 1$. This property is reminiscent of the approach adopted within the linear model in Ref. [7], where the mean field is the average terrace width (and thus coincides with the initial width for a vicinal crystal). By contrast, in our nonlinear setting the approximation $f \approx 1$ can only be justified in the limit of strong enough step interactions ($g \gg 1$).

In this case, deviations of the terrace widths from their average (and initial, deterministic) values become energetically unfavorable, and step fluctuations tend to be suppressed.

Based on these observations, we fix $g \gg 1$ and enforce a closure for Eqs. (29) and (30) via the *ansatz* $p^{(3)}(s, y_1, y_2) \approx P(s)P(y_1)P(y_2)$. For independent terraces moving in an “external potential” (i.e., loosely speaking, a force field *not* related to neighboring terraces), this expression becomes exact. In the presence of step interactions, this approximation is reasonable as will be shown by comparison to kMC simulations. Step correlations are *ipso facto* not included in our MF scheme. Accordingly, in our asymptotic calculations we assume that corrections resulting from terrace-terrace correlations are of order less than $O(g^{-1})$. In Sec. VII we further discuss this assumption.

Accordingly, Eq. (30) becomes (with $\partial_t \equiv 0$)

$$A(s, f) \approx \int_{\mathbb{R}_2^+} \tilde{A}(s, y_1, y_2) P(y_1)P(y_2) dy_1 dy_2, \quad (31)$$

where $\tilde{A}(s, y_1, y_2) = A(y_2, y_1, s, y_1, y_2)$ (cf. Eq. (11)), and

$$A(s, f) = \left[\frac{4}{s+c} + \frac{2}{f(s)+c} \right] \left[\frac{1}{s^3} - \frac{1}{f(s)^3} \right],$$

$$\tilde{A}(s, y_1, y_2) = \frac{4}{c+s} \left[\frac{1}{s^3} - \frac{1}{y_1^3} \right] - \frac{2}{c+y_1} \left[\frac{2}{y_1^3} - \frac{1}{y_2^3} - \frac{1}{s^3} \right].$$

Recall that $c = \check{c}/\langle w \rangle$ expresses the interplay of adatom diffusion and attachment-detachment (see Sec. II). Here, by abusing notation, we set $f(s) = f(s, t \rightarrow \infty)$ assuming $f(s, t)$ settles to a steady state.

To enable analytical treatment, we apply the *ansatz*

$$f(s) = f_0 + g^{-\alpha} f_1(s) + o(g^{-\alpha}), \quad (32)$$

where $\alpha > 0$ is determined below to be 1, and $f_0 = \mathcal{O}(1)$ is a *constant* independent of g in anticipation of a uniform mean field in the limit of strong interactions. Equation (32) is viewed as a formal expansion for $f(s)$ when g is large within our decorrelation *ansatz*. In the same vein, we expand the TWD as

$$P(s) = P_0(s; g) + g^{-\alpha} P_1(s; g) + o(g^{-\alpha}). \quad (33)$$

In this expansion, we indicate that the coefficients P_k (where k denotes the expansion order) may depend on g . This distinction is made for later convenience, since the P_k bear a g -dependence of exponential type.

Our next task is to solve Eq. (31) in light of expansions (32) and (33). If the TWD is sharply peaked at, say, $s = \zeta$, and decays rapidly to zero away from ζ , then Eq. (31) can be simplified via asymptotics [30]. Thus, we expand $\tilde{A}(s, y_1, y_2)$ about $y_1 = y_2 = \zeta$. Recall that the

analysis of Sec. III indicates that, for $g \gg 1$, the standard deviation of the (Gaussian within the linear model) TWD is $O(g^{-1/2})$. This scaling with g of the standard deviation should also hold for the present case since the linear analysis is reasonably valid near the TWD peak.

Next, we comment on ζ . By setting $\partial_t P(s, t) = 0$ in Eq. (22), we obtain

$$P''(s) = \frac{g}{3} \times \left[\left(\frac{4}{c+s} + \frac{2}{c+f(s)} \right) \left(\frac{1}{s^3} - \frac{1}{f(s)^3} \right) P(s) \right]', \quad (34)$$

where the prime here denotes differentiation with respect to s , e.g., $P'(s) = dP(s)/ds$. With $P(s) \geq 0$, we have $P''(\zeta) < 0$ and $P'(\zeta) = 0$ when $\zeta = f(\zeta)$ (which defines the maximum of P).

The substitution of formulas (32) and (33) into Eq. (31) along with the Taylor expansion of $A(s, y_1, y_2)$ around $y_1 = y_2 = \zeta$ yield the expression

$$\begin{aligned} & \left[\frac{4}{c+s} + \frac{2}{c+f_0} \left(1 - \frac{f_1(s)}{g^\alpha(c+f_0)} + \dots \right) \right] \\ & \times \left[\frac{1}{s^3} - \frac{1}{f_0^3} \left(1 - \frac{3f_1(s)}{g^\alpha f_0} + \dots \right) \right] = \\ & \int_{\mathbb{R}_2^+} dy_1 dy_2 P(y_1)P(y_2) \\ & \times \left\{ \frac{4}{s+c} \left[\frac{1}{s^3} - \frac{1}{f_0^3} + \frac{3(y_1-f_0)}{f_0^4} - \frac{12(y_1-f_0)f_1(\zeta)}{g^\alpha f_0^5} + \dots \right] \right. \\ & + 2 \left[\frac{1}{c+f_0} - \frac{y_1-f_0}{(c+f_0)^2} + \frac{2f_1(\zeta)(y_1-f_0)}{g^\alpha(c+f_0)^3} + \dots \right] \\ & \times \left[\frac{1}{s^3} - \frac{1}{f_0^3} + \frac{3[2(y_1-f_0) - (y_2-f_0)]}{f_0^4} \right. \\ & \left. \left. - \frac{12f_1(\zeta)}{g^\alpha f_0^5} [2(y_1-f_0) - (y_2-f_0)] + \dots \right] \right\}, \quad (35) \end{aligned}$$

which, by dominant balance [33] in g , leads to a cascade of equations for f_k . In deriving Eq. (35), we made extensive use of the binomial expansion, $(1+z)^\varsigma = 1 + \zeta z + \dots$ ($|z| < 1$, $\varsigma \in \mathbb{R}$), as well as of the expansion for $f(\zeta)$ by Eq. (32). Note that expanding A gives rise to terms $(y_{1,2} - f_0)^n$, $n = 1, 2, \dots$, which yield an *implicit* dependence on g through the associated moments of P . A crucial goal with the perturbation scheme is to determine the expansion order in g of these moments. This in turn determines α .

By virtue of Eqs. (32) and (33), Eq. (22) entails

$$\begin{aligned} & \frac{d^2}{ds^2} \left[P_0(s) + \frac{P_1(s)}{g^\alpha} + \dots \right] \\ &= \frac{g}{3} \frac{d}{ds} \left\{ \left(\frac{4}{c+s} + \frac{2}{c+f_0} - \frac{2f_1(s)}{g^\alpha(c+f_0)^2} + \dots \right) \right. \\ & \quad \times \left(\frac{1}{s^3} - \frac{1}{f_0^3} + \frac{3f_1(s)}{g^\alpha f_0^4} + \dots \right) \\ & \quad \left. \times \left[P_0(s) + \frac{P_1(s)}{g^\alpha} + \dots \right] \right\}. \end{aligned} \quad (36)$$

Equations (35) and (36) form the basis of our approximation scheme for $f(s)$ and $P(s)$.

B. Zeroth-order approximation and composite expression

In this subsection, we outline the procedure for solving the system of Eqs. (35) and (36) up to some order in g . Our discussion can be extended to the time-dependent case, which is the focus of Sec. VI.

By dominant balance, from Eq. (35) we obtain an $O(g^0)$ equation for f_0 :

$$\begin{aligned} A(s, f_0) = \int_0^\infty P(y_1) \left\{ A(s, f_0) + (y_1 - f_0) \left[\frac{12}{f_0^4(s+c)} \right. \right. \\ \left. \left. - \frac{2}{(c+f_0)^2} \left(\frac{1}{s^3} - \frac{1}{f_0^3} \right) + \frac{6}{f_0^4(c+f_0)} \right] \right\} dy_1 \end{aligned} \quad (37)$$

Recall that $P(y)$ is normalized and has unit mean. Thus, Eq. (37) reduces to

$$\int_0^\infty P(y_1)(y_1 - f_0) dy_1 = 0, \quad (38)$$

which readily implies $f_0 = 1$.

By Eq. (36) with $f_0 = 1$, the zeroth-order TWD, $P_0(s)$, satisfies the differential equation

$$P_0''(s) = \frac{g}{3} \left[\left(\frac{4}{c+s} + \frac{2}{c+1} \right) \left(\frac{1}{s^3} - 1 \right) P_0(s) \right]', \quad (39)$$

subject to boundary conditions (23b). Equation (39) is integrated directly to give

$$\begin{aligned} P_0(s; g) = \mathcal{N}_0 \frac{s^{\frac{4g}{3c^3}}}{(s+c)^{\frac{4g}{3}(\frac{1}{c^3}+1)}} \\ \times \exp \left[-\frac{2gs}{3(c+1)} + \frac{4g}{3c^2s} - \frac{g(3c+2)}{3c(c+1)s^2} \right], \end{aligned} \quad (40)$$

where $\mathcal{N}_0(g, c)$ is a normalization constant (see Appendix B). A noteworthy feature of this P_0 , called ZO in figures, is an essential singularity at $s = 0$, which forces P_0 and *all* its derivatives to *vanish* as $s \rightarrow 0^+$. This singularity is viewed as an artifact connected to the 1D

character of the present model. As mentioned earlier, moments derived from Eq. (40) contain a g dependence, which by dominant balance affects the cascade of equations produced by Eq. (35).

We turn our attention to the variance, σ_0^2 , associated with $P_0(s; g)$. In Appendix B we show that, for large g ,

$$\sigma_0^2 = \frac{c+1}{6g} + o(g^{-1}). \quad (41)$$

The leading-order term of this formula is consistent with the long-time limit of the variance for the linearized model; cf. Eq. (19) with $g_c = 3g/(c+1)$.

Next, we determine the α entering expansions (32) and (33). By Eq. (35), the value of α comes from balancing the $\mathcal{O}(g^{-\alpha})$ term on the left-hand side with the $\mathcal{O}(g^{-1})$ term from the variance of P_0 , σ_0^2 , on the right-hand side. Thus, we find $\alpha = 1$.

Next we focus on $f_1(s)$, the coefficient of the $\mathcal{O}(g^{-1})$ term in the expansion for f . By use of Eqs. (35) and (41), we obtain the formula

$$\begin{aligned} f_1(s) = -\frac{c+1}{3} \\ \times \left[\frac{12}{s+c} + \frac{6}{c+1} + \frac{6}{(c+1)^2} - \frac{1}{(c+1)^3 s^3} + \frac{1}{(c+1)^3} \right] \\ \div \left[\frac{12}{s+c} + \frac{6}{c+1} - \frac{2}{(c+1)^2 s^3} + \frac{2}{(c+1)^2} \right]. \end{aligned} \quad (42)$$

We add in passing that the location $\zeta = f(\zeta)$ of the TWD maximum cancels to $\mathcal{O}(g^{-1})$ in Eq. (35), and thus does not appear in expressions (38)–(42).

We choose not to compute $P_1(s)$ explicitly. The form of the requisite $f_1(s)$ is already complicated, rendering further computations for P unwieldy. Instead, we resort to Eq. (22) with $\dot{P} = P$, $\partial_t P \equiv 0$, $f(s) \approx 1 + f_1(s)/g$ and $\hat{q} = \sqrt{6}$. By direct integration we derive a “composite expression” for $P(s)$, called CE in figures, which is valid to $\mathcal{O}(g^{-1})$:

$$P(s) \approx \mathcal{N}(g, c) \exp \left[\frac{g}{3} \int_1^s A \left(z, 1 + \frac{f_1(z)}{g} \right) dz \right], \quad (43)$$

where $f_1(s)$ is given by Eq. (42), and $\mathcal{N}(g, c)$ is a normalization constant subject to $\int_0^\infty P(s) ds = 1$.

We conclude this section with a few remarks on Eqs. (40) and (43). These forms are *different* from the generalized Wigner surmise, $P(s) \propto s^e e^{-b_e s^2}$, invoked for surface systems, e.g., in Ref. [6]. For small positive s , $P_0(s)$ here exhibits an (integrable) essential singularity at $s = 0$, which mathematically prohibits having nonzero values for negative terrace widths, $s < 0$. This behavior does not harm the moments of P_0 . It is intimately related to the 1D character of our model and is not expected to persist in 2D step configurations. Note that, for large values of s , $P_0(s) \sim \mathcal{N}_0 s^{-4g/3} e^{-\frac{2g}{3(c+1)}s}$. For further discussion, see Sec. VII.

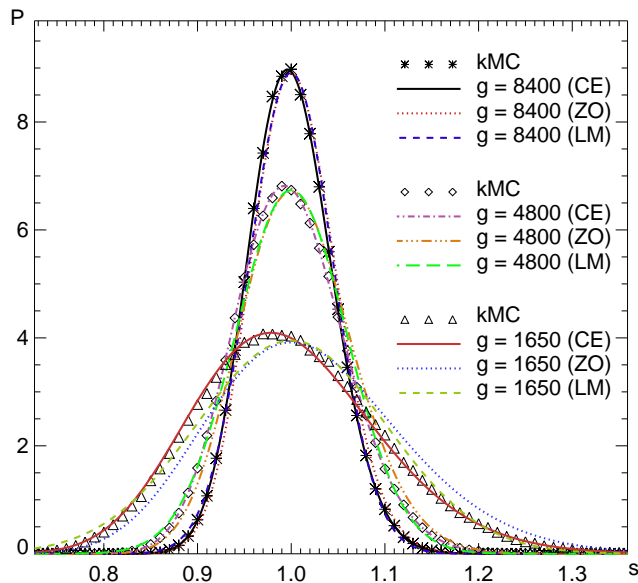


FIG. 2. (Color online) Steady-state TWD, $P(s)$, by: kMC simulations; and MF zeroth-order (ZO) approximation (40), MF composite expression (CE) (43), and linearized model (LM) according to Eq. (20) for $g = 1650, 4800, 8400$ and $c = 100$.

In Fig. 2 we plot our MF zeroth-order approximation and composite expression vs. the analytical prediction of the linearized model (Sec. III) and 1D kMC simulations for the TWD at sufficiently long times. By comparison, we see that (i) the MF composite expression (43) for $P(s)$ follows the kMC-produced TWD more closely than the MF zeroth-order formula (40) even as g decreases; and (ii) the TWD generated from the linearized model starts to deviate from the kMC results for smaller g , in contrast to the MF prediction.

Notably, the correction $f_1(s)/g$ to the mean field f has a singularity in the interval $(0, 1/2)$ for s , as can be shown from Eq. (42) via algebraic inequalities. This singularity does not cause any pathology to the moments associated with P , and is viewed as a consequence of asymptotic approximations leading to Eq. (35). For $g \gg 1$, this singularity lies far away from the location of the TWD peak, and the MF correction $f_1(s)$ improves the accuracy for $P(s)$ by Eq. (43) (see Fig. 2). In fact, the inclusion of $f_1(s)$ shifts the TWD peak to the left, thus producing good agreement of the MF approximation, Eq. (43), with the kMC simulation.

VI. TIME-DEPENDENT TWD

In this section, we derive an approximation for the TWD for times $t > 0$ by invoking a time-dependent mean field, $f(s, t)$. First, we introduce asymptotic expansions and an appropriate scaling of time in order to simplify Eqs. (22) and (29). Second, we solve approximately the

requisite equations for the time-dependent TWD and f .

A. Formulation and asymptotics

Our formulation relies on extending the main hypotheses of Sec. V (for the steady state) to the present, time-dependent setting under $g \gg 1$. So, we assume that for finite times the strong step interactions suppress terrace fluctuations, cause narrowing of the TWD, and favor terrace decorrelation.

Once again, the starting point is a formal expansion of the mean field, f , in powers of g :

$$f(s, t) = f_0 + g^{-\alpha} f_1(s, t) + o(g^{-\alpha}), \quad (44)$$

where the exponent α ($\alpha > 0$) is again to be determined. We write the time-dependent TWD in the factorized form

$$P(s, t) = P_s(s, t) \psi(s, t), \quad (45)$$

$$P_s(s, t) = \mathcal{N}(g, c) \exp \left[\frac{g}{3} \int_1^s A(z, f(z, t)) dz \right], \quad (46)$$

where $\psi(s, t)$ is to be determined; cf. Eq. (43) for the steady-state TWD [31].

Equation (45) is a generalization of Eq. (43) for the steady state. The time variation in $P_s(s, t)$ enters through the mean field (Sec. VI B). The function $P_s(s, t)$ is invoked for two reasons: (i) it ensures that the time-dependent TWD can satisfy boundary conditions (23b); and (ii) P_s manifestly decays to the steady-state TWD (43) as $t \rightarrow \infty$. This latter property implies the additional requirement that $\psi(s, t) \rightarrow 1$ as $t \rightarrow \infty$.

Ansatz (45) along with Eq. (46) transform Eq. (22) into a partial differential equation for $\psi(s, t)$:

$$3\partial_{ss}\psi(s, t) + gA(s, f(s, t))\partial_s\psi(s, t) = \partial_t\psi(s, t) + P_s^{-1}\psi(s, t)\partial_t P_s. \quad (47)$$

Our next task is to determine $\psi(s, t)$ approximately via Eq. (47) when g is large.

In light of our findings for the linearized model (Sec. III), we need to *reconsider* the use of variables (s, t) in the equations of motion. Suppose that we invoke the formal expansion

$$\psi(s, t) = \psi_0(s, t) + g^{-\gamma}\psi_1(s, t) + o(g^{-\gamma}), \quad (48)$$

where $\psi_k(s, t)$ are $\mathcal{O}(1)$ coefficients, and γ will be determined to be $1/2$. Then, we obtain an equation cascade for ψ_k that fails to capture essential features of the time-dependent TWD in correspondence to the linear case (Sec. III): the natural scaling of time t with g in the variance is missed.

For a procedure of determining $\psi(s, t)$ consistent with the analysis of the linear model, we need to scale the space and time variables (see Eq. (19), for instance). Accordingly, by dividing Eq. (47) by g and defining

$$\xi = \sqrt{g}(s - 1), \quad \tau = 3gt,$$

we obtain an equation for $\tilde{\psi}(\xi, \tau) \equiv \psi(s(\xi), t(\tau))$:

$$\begin{aligned} \partial_{\xi\xi}\tilde{\psi}(\xi, \tau) + \frac{\sqrt{g}}{3}A\left(1 + \frac{\xi}{g^{1/2}}, \tilde{f}(\xi, \tau)\right)\partial_{\xi}\tilde{\psi}(\xi, \tau) \\ = \partial_{\tau}\tilde{\psi}(\xi, \tau) + \frac{1}{P_s}\tilde{\psi}\partial_{\tau}P_s, \end{aligned} \quad (49)$$

where $\tilde{f}(\xi, \tau) \equiv f(s(\xi), t(\tau))$. For ease of notation, we henceforth drop the tildes for ψ and f , writing, e.g., $\psi(\xi, \tau)$. The variables ξ and τ simplify the analysis. For instance, in the computation of moments of the TWD the major contribution to integration comes a region where $\xi = \mathcal{O}(1)$. In s , this region is within a vicinity of width $\mathcal{O}(g^{-1/2})$ around the location of the TWD peak.

Taking into account the scaled spacetime variables, we now write

$$\psi(\xi, \tau) = \psi_0(\xi, \tau) + g^{-\gamma}\psi_1(\xi, \tau) + o(g^{-\gamma}). \quad (50)$$

To complete the formulation of the MF system, we need to state the corresponding equation for $f(\xi, \tau)$. An inspection of calculations leading to Eq. (35) reveals that this formula also holds in the time-dependent case (by replacement of $f(s)$ with $f(\xi, \tau)$). As noted above, an assumption underlying our approximations is that terrace correlation effects are less than $\mathcal{O}(g^{-1})$ for all $t > 0$. Further discussion of this point is deferred to Sec. VII.

B. Approximate time-dependent TWD

The rationale for determining the TWD P as a function of (ξ, τ) does not essentially differ from the rationale of Sec. V. In particular, our previous conclusion that $f_0 = 1$ for the steady state relies only on the fixed-system-size requirement and normalization of the TWD. These conditions are enforced in the time-dependent case as well. Hence, we conclude that $f_0 = 1$ in the present case.

We proceed to compute $\psi_0(\xi, \tau)$. By substituting Eq. (50) into Eq. (49) and properly expanding the term $A(1 + \xi/g^{1/2}, f(\xi, \tau))$, we find

$$\begin{aligned} \partial_{\xi\xi}\left[\psi_0(\xi, \tau) + \frac{\psi_1(\xi, \tau)}{g^{\gamma}} + \dots\right] + \left[\frac{6\xi}{c+1} + \mathcal{O}(g^{-1/2})\right] \\ \times \partial_{\xi}\left[\psi_0(\xi, \tau) + \frac{\psi_1(\xi, \tau)}{g^{\gamma}} + \dots\right] \\ = \partial_{\tau}\left[\psi_0(\xi, \tau) + \frac{\psi_1(\xi, \tau)}{g^{\gamma}} + \dots\right] \\ + \frac{1}{P_s}(\partial_{\tau}P_s)\left[\psi_0(\xi, \tau) + \frac{\psi_1(\xi, \tau)}{g^{\gamma}} + \dots\right]. \end{aligned} \quad (51)$$

Note the $\mathcal{O}(g^{-1/2})$ correction stemming from the definition of ξ . By dominant balance, Eq. (51) yields $\gamma = 1/2$. Given that $f_0 = 1$ we infer that the time derivative of P_s does not contribute to leading order in g . Thus, we obtain the zeroth-order equation

$$\partial_{\xi\xi}\psi_0(\xi, \tau) - \frac{6\xi}{c+1}\partial_{\xi}[\psi_0(\xi, \tau)] = \partial_{\tau}\psi_0(\xi, \tau), \quad (52)$$

which is subject to the initial condition $P_s(\xi, 0)\psi(\xi, 0) = \delta(\xi)$ (cf. Eqs. (23a) and (45)). After multiplying both sides of Eq. (52) by $\exp[-3\xi^2/(c+1)]$, we derive the solution [32]

$$\begin{aligned} \psi_0(\xi, \tau) = \left(\frac{6g}{c+1}\right)^{1/2} P_s(1, 0)^{-1} [2\pi \left(1 - e^{-\frac{12\tau}{c+1}}\right)]^{-1/2} \\ \times \exp\left[-\frac{3\xi^2 e^{-\frac{12\tau}{c+1}}}{(c+1)(1 - e^{-\frac{12\tau}{c+1}})}\right]. \end{aligned} \quad (53)$$

A corresponding formula for the TWD follows from Eq. (45) with $f_0 = 1$.

Next, we focus on corrections to the mean field $f_0 = 1$. The methodology to derive f_1 in the steady state applies here as well, independently of the scaling of s and t with powers of g . In fact, the spatial dependence of f_1 remains intact, but it is multiplied by a τ -dependent variance (see Eq. (54)). Accordingly, technically speaking, the use of variables (ξ, τ) for f introduces an explicit dependence of f_1 on g . By recourse to Eqs. (35) and (42), we find

$$\begin{aligned} f_1 = -2g\sigma_0(\tau)^2 \\ \times \left[\frac{12}{s+c} + \frac{6}{c+1} + \frac{6}{(c+1)^2} - \frac{1}{(c+1)^3 s^3} + \frac{1}{(c+1)^3}\right] \\ \div \left[\frac{12}{s+c} + \frac{6}{c+1} - \frac{2}{(c+1)^2 s^3} + \frac{2}{(c+1)^2}\right] \end{aligned} \quad (54)$$

which follows from the steady-state case. Here, $s = 1 + g^{-1/2}\xi$, $t = (3g)^{-1}\tau$ and $\sigma_0^2(\tau)$ is the variance for the TWD $P(s, t)$ of Eq. (45) under $\psi \approx \psi_0$ and Eq. (46) with $f \approx f_0 = 1$. By the same method used to derive Eq. (41), one finds

$$\sigma_0(\tau)^2 = \frac{c+1}{6g} \left(1 - e^{-\frac{12\tau}{c+1}}\right). \quad (55)$$

In the limit $t \rightarrow \infty$, this result agrees with both the MF steady-state variance, Eq. (41), and the variance from the linearized model, Eq. (19).

In Fig. 3, we plot the variance as a function of time using different approximation schemes, i.e., the linearized model and the MF scheme, compared with kMC simulations. We observe that the MF approximation for the variance approaches a finite limit (in steady state) at nearly the same time as the kMC simulation, with improved accuracy for larger g . By contrast, the linearized model predicts a slower approach to steady state. In Fig. 4, we show plots of the time-dependent TWD for some fixed, intermediate time t .

Qualitatively, then, the TWD evolves as follows: For sufficiently small times, the TWD is approximately Gaussian, due to the delta-function initial condition, affected slightly by an asymmetric contribution from the steady state. As time increases, the asymmetry becomes more pronounced, and the Gaussian behavior gives way to the steady state, Eq. (40). Simultaneously, the correction f_1

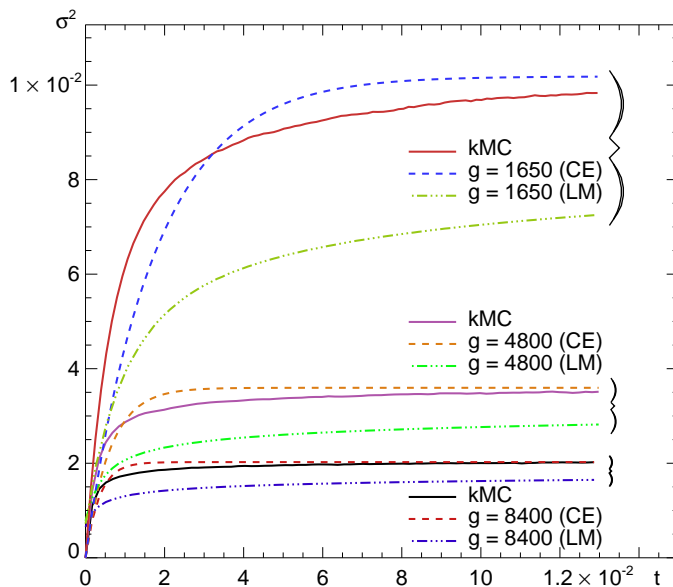


FIG. 3. (Color online) Variance of TWD as a function of dimensionless time by: kMC simulations; integration of MF composite expression (CE) (45) with Eq. (46) and $f = f_0 + f_1/g$, and Eq. (19) of linearized model (LM), for $g = 1650, 4800, 8400$ and $c = 100$. For stronger step interactions (lower part of figure), the TWD becomes narrower.

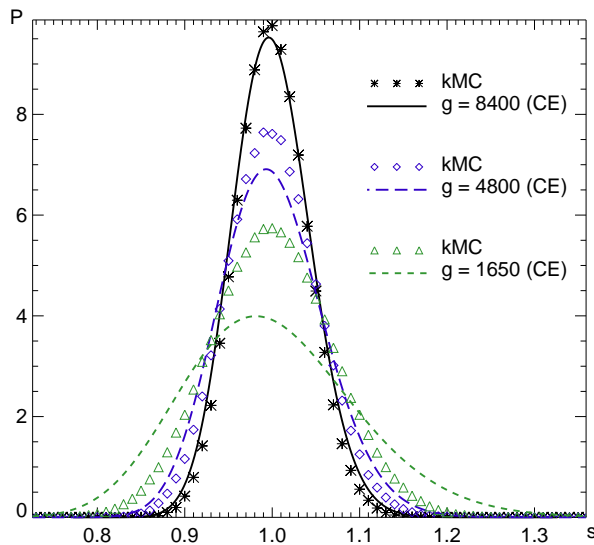


FIG. 4. (Color online) Time-dependent TWD as a function of terrace width variable, s , for fixed intermediate time t by: kMC simulations; and MF time-dependent composite expression (CE) by Eq. (45) with Eq. (46) and $f = f_0 + f_1/g$ for $g = 1650, 4800, 8400$ with $c = 100$. In kMC simulations, the TWD is computed after 2500 iterations of the algorithm; and values of b are fit to the steady-state TWD (see Appendix C).

to the average value $f_0 = 1$ grows larger, causing a consistent shift of the peak of the TWD to the left (see Eqs. (43) and (54)).

VII. DISCUSSION

Our main goal in this paper is the development of analytical techniques for the approximate solution of stochastic equations for fluctuations of steps on vicinal surfaces. A crucial quantity is the TWD. To enable some analytical treatment of the governing equations, we restrict attention to 1D geometries.

The starting step-flow model and approximation schemes are amenable to direct extensions in 1D. For example, the effect of material deposition can be included in the step motion laws. In this case, the increase of deposition flux causes narrowing of the TWD [7] and, hence, contributes qualitatively in a fashion similar to an increase in the step interaction strength, g . Further, a contribution to the noise terms stems from fluctuations in the number of deposited atoms [34]. The joint effect of deposition and dipolar step interactions is expected to result in an asymmetry of the TWD (in s), in contrast to the Gaussian TWD found via a linearized model in Refs. [7, 10]. Richer kinetics such as evaporation and step permeability [35] can be included in the formulation.

Our model and analysis have limitations. A fundamental question is to what extent our 1D model can be connected to the 2D dynamics of actual surfaces, and hence for which observable phenomena it can account. One indication of the inadequacy of the 1D model to fully describe 2D step fluctuations is the appearance of a singularity of the TWD, $P(s)$, at zero terrace width ($s = 0$). Since this singularity is integrable, it does not cause any problems in computing the moments of P . Furthermore, this behavior forces the TWD and all its space derivatives to vanish as the terrace width approaches zero. However, step meandering in 2D is expected to “regularize” the behavior of the TWD near $s = 0$.

We make use of formal expansions in negative powers of the interaction strength, g , after we apply a decorrelation ansatz for terraces. The modification of the FPE for the TWD by terrace correlation effects is not considered here. To include correlations, one needs to update the 5-terrace joint probability density via the corresponding evolution equation of the BBGKY hierarchy and possible application of a partial decorrelation ansatz. This task is left for near-future work.

Despite the above limitations, our analysis could be useful in understanding quantitative features of certain quasi-1D step systems similar to those in Refs. [3, 36]. The time dependent, composite TWD (45) expresses the interplay between mass transport and step interactions via parameters c and g , respectively. Hence, for systems in which step-step interactions are the dominant force driving evolution [3], fitting experimental data with Eq. (43) should indicate the mass transport mechanism

via the expression $c = D\langle w \rangle^{-1}/(k_-^{-1} + k_+^{-1})$, as well as the interaction parameter g .

We expect that our analysis is also useful in understanding more general, qualitative features of 2D step systems. The underlying hypothesis of statistical independence would reasonably hold for smooth steps in 2D. Thus, it is conceivable that our technique and MF predictions are reasonably applicable to 2D geometries. For example, the asymmetry of the TWD because of step interactions, as well as the narrowing of the TWD with the increase of the step interaction strength, g , should persist in 2D. In particular, our prediction that the terrace width variance scales as $1/g$ should hold in a 2D setting.

It should be stressed, however, that modeling noise in 2D introduces subtle issues and more elaborate governing equations [4, 5]. Reconciling the BCF picture with noise in 2D is a largely unexplored area. In the same vein, an issue not addressed here is the possible dependence of the diffusion coefficient on the terrace width in 1D. This would require choosing between, e.g., Stratonovich and Itô stochastic calculus [15]. Our relatively simple model of noise circumvents this complication.

Our analysis shows in a *minimal setting* how the mean field, f , necessary to decouple the stochastic equations of motion is influenced by *nonlinearities* stemming from the step interaction energy. Because of the interaction, the self-consistent mean field does *not* in principle coincide with the average terrace width. In fact, corrections for this f beyond the terrace width average are shown here to be important. In this vein, the use of a linearized model has shortcomings, which we detect via comparisons with kMC simulations.

It is tempting to compare our analytical results for the steady-state TWD to previous proposals involving the generalized Wigner surmise, $P(s) \propto s^\rho e^{-b_\rho s^2}$; see, e.g., [6]. Within the 1D model studied here, our computed TWD resembles qualitatively the Wigner surmise for large enough values of the step-step interaction strength, when both TWDs tend to become symmetric; see Fig. 5. Further comparisons motivate the use of a 2D geometry and lie beyond our present scope.

Our analysis brings forth a close relationship between step flow SDEs and kMC method in 1D. In Ref. [7] the authors compare qualitatively the prediction of a linear 1D stochastic model with 2D kMC simulations when there is material deposition. Our work indicates a more direct, quantitative relation between the two approaches (analytical and kMC one), since the corresponding models are both 1D.

VIII. CONCLUSION

In this paper, we formulated and analyzed a 1D stochastic model of interacting steps on a vicinal crystal. The starting point was the BCF theory, enriched with elastic-dipole step interactions and ad hoc conservative white noise. First, we linearized the governing equations

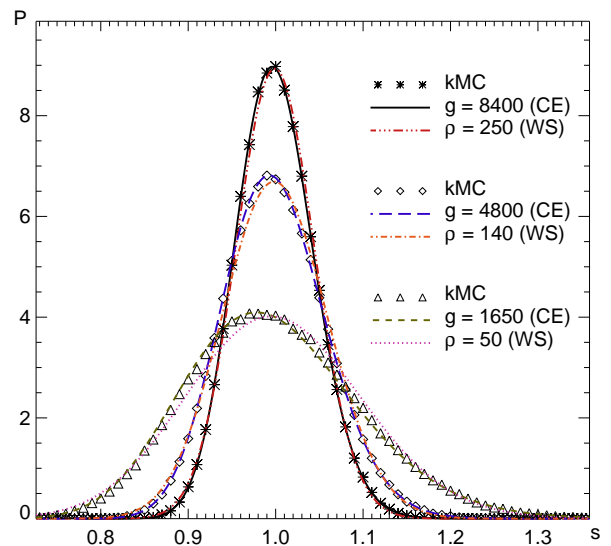


FIG. 5. (Color online) Predictions for TWD: mean-field CE given in Eq. (43), and generalized Wigner surmise (WS), $P(s) = \mathcal{N}_\rho s^\rho e^{-b_\rho s^2}$ (\mathcal{N}_ρ : normalization constant); the coefficient b_ρ provides unit mean [6].

of terrace motion and derived the TWD for the resulting, coupled system of SDEs. Second, by perturbation theory for strong step interactions, we considered the effect of nonlinearities by employing, within a terrace decorrelation hypothesis, a MF formalism that decouples the SDEs. Our analysis of the TWD indicated a rich behavior not fully captured by the linearized system. Third, we compared the analytical predictions with 1D kMC simulations and indicated how our model may be used to determine physical parameters of quasi-1D systems. Open questions concern the application of MF approximations to 2D stochastic step flow models, and analysis of terrace correlation effects and terrace-width-dependent noise.

ACKNOWLEDGMENTS

The authors thank Professors M. E. Fisher, J. Krug, C. D. Levermore, A. Pimpinelli, A. E. Tzavaras, and J. D. Weeks for useful discussions. Work by PP and TLE was supported by the NSF MRSEC under Grant DMR 0520471 at the University of Maryland, with ancillary support from CNAM. DM's work was supported by NSF under Grant DMS 0847587.

Appendix A: On circulant matrices

In this appendix, we derive Eq. (16) in detail on the basis of standard theory for circulant matrices. For any

square, circulant matrix \mathbf{M} , we apply the formula [37]

$$\begin{aligned} |e^{\mathbf{M}}|^2 &= \frac{1}{N} \text{tr}[(e^{\mathbf{M}})^T e^{\mathbf{M}}] = \frac{1}{N} \text{tr}[e^{\mathbf{M}^T + \mathbf{M}}] \\ &= \frac{1}{N} \sum_{k=0}^{N-1} e^{\lambda_k}, \end{aligned} \quad (\text{A1})$$

where tr denotes the trace and λ_k are the eigenvalues of the matrix $\mathbf{M}^T + \mathbf{M}$, taking into account that circulant matrices *commute*. Thus, it would be desirable to determine an \mathbf{M} such that $\mathbf{X}e^{\mathbf{Y}} \equiv e^{\mathbf{M}}$.

Specifically, now consider the quantity in question,

$$|\mathbf{X}e^{\mathbf{Y}}|^2 = N^{-1} \text{tr}[\mathbf{X}\mathbf{X}^T e^{\mathbf{Y}^T + \mathbf{Y}}], \quad (\text{A2})$$

where \mathbf{X}, \mathbf{Y} are square, circulant matrices. Because $\widetilde{\mathbf{X}} = \mathbf{X}\mathbf{X}^T$ is symmetric and circulant, its eigenvalues ϑ_j are

$$\vartheta_j = F_{j,k} \widetilde{\mathbf{X}}_{k,0}, \quad j = 1, \dots, N, \quad (\text{A3})$$

where $\mathbf{F} = [F_{j,k}]$ is the discrete Fourier transform matrix, whose elements are $F_{j,k} = \exp[-2\pi i(jk)/N]$. Since $\widetilde{\mathbf{X}}_{0,k} = \widetilde{\mathbf{X}}_{0,N-k}$, the eigenvalues ϑ_j are real.

Next, we compute the logarithm of $\widetilde{\mathbf{X}}$ by the formula [38]

$$\ln(\widetilde{\mathbf{X}}) = \mathbf{F} \ln(\mathbf{F}^{-1} \widetilde{\mathbf{X}} \mathbf{F}) \mathbf{F}^{-1},$$

where $\mathbf{F}^{-1} \widetilde{\mathbf{X}} \mathbf{F} = \text{diag}(\vartheta_k)$, a diagonal matrix. Since this last matrix is diagonal, taking its logarithm amounts to taking the logarithm of its diagonal elements. For complex eigenvalues, we consider the principal branch of the logarithm for definiteness [39]. Furthermore, we assert (trivially) that $\ln(\widetilde{\mathbf{X}})$ is circulant.

Thus, we have

$$\widetilde{\mathbf{X}} e^{\mathbf{Y}^T + \mathbf{Y}} = e^{\ln(\widetilde{\mathbf{X}}) + \mathbf{Y}^T + \mathbf{Y}}. \quad (\text{A4})$$

In view of Eq. (A1) with $\mathbf{M} = e^{\ln(\widetilde{\mathbf{X}}) + \mathbf{Y}}$, we infer that

$$\begin{aligned} |\mathbf{X}e^{\mathbf{Y}}|^2 &= N^{-1} \text{tr}[\mathbf{X}\mathbf{X}^T e^{\mathbf{Y}^T + \mathbf{Y}}] \\ &= \frac{1}{N} \sum_{k=0}^{N-1} e^{\ln(\vartheta_k) + \lambda_k} = \frac{1}{N} \sum_{k=0}^{N-1} \vartheta_k e^{\lambda_k}. \end{aligned}$$

Appendix B: Computations of variance

In this appendix, we compute the variances of: (i) the linearized model by Eq. (19); and (ii) the leading-order MF TWD from Eq. (40). We also show that a first-order scheme for a conservative noise in the linearized model leads to an unbounded variance. Further, we compute the normalization constant $\mathcal{N}_0 = \mathcal{N}_0(g, c)$ introduced in Eq. (40).

1. Linearized model

a. Second-order conservative noise

Consider Eq. (19), which stems from the circulant diffusion coefficient $\mathbf{Q} = [Q_{j,k}]$ with first row $[2, -1, 0, \dots, 0, -1]$. We now derive an asymptotic formula for $g_c t \gg 1$. The major contribution to integration arises from the endpoints $y = 0, 1$. Thus, we have

$$\begin{aligned} \sigma_{\text{lin}}^2(t) &\sim \frac{1}{2g_c} \left[1 - \int_{-\infty}^{\infty} e^{-32\pi^4 g_c t y^4} dy \right] \\ &= \frac{1}{2g_c} \left[1 - \frac{\Gamma(1/4)}{2^{9/4}\pi} (g_c t)^{-1/4} \right], \end{aligned} \quad (\text{B1})$$

where $\Gamma(z)$ is the usual Gamma function [40].

Alternatively, we can evaluate $\sigma_{\text{lin}}^2(t)$ exactly in terms of series involving modified Bessel functions, $I_l(z)$. Specifically, by making use of the relation [32]

$$e^{z \cos \theta} = I_0(z) + 2 \sum_{l=1}^{\infty} I_l(z) \cos(l\theta),$$

where $0 \leq \theta < 2\pi$, and the orthogonality of trigonometric functions, we obtain

$$\begin{aligned} \sigma_{\text{lin}}^2(t) &= \frac{1}{2g_c} - e^{-12g_c t} \left[I_0(16g_c t) I_0(-4g_c t) \right. \\ &\quad \left. + \sum_{l=1}^{\infty} I_{2l}(16g_c t) I_l(-4g_c t) \right]. \end{aligned} \quad (\text{B2})$$

This expression is particularly useful for $0 < g_c t \ll 1$, since $I_l(z) = \mathcal{O}(z^l)$ as $z \rightarrow 0$ and the above series provides a MacLaurin-type expansion. Note that formula (B2) may not be used for $g_c t \gg 1$; direct recourse to asymptotic formula (B1), and possibly higher-order terms, is advisable in this case.

b. First-order conservative noise and divergence

We now show that when the diffusion coefficient \mathbf{Q} entering SDEs (13) is the circulant matrix with first row $[1, -1, 0, 0, \dots]$, the corresponding variance for any terrace diverges as $\mathcal{O}(t^{1/4})$ in the limit $t \rightarrow \infty$. To derive this result, we make use of Eq. (16) and let $N \rightarrow \infty$. We then evaluate the variance asymptotically for large $g_c t$.

The matrix $\widetilde{\mathbf{Q}} = \mathbf{Q}\mathbf{Q}^T$ is circulant and has first row $[2, -1, 0, \dots, 0, -1]$; the eigenvalues are computed by $\vartheta_k = F_{k,l} \widetilde{Q}_{l,0}$ where $F_{k,l} = \exp[-2\pi i(kl)/N]$ (see Appendix A). Recall that the \mathbf{A} entering Eq. (13) is circulant, and its first row is $[6, -4, 1, 0, \dots, 0, 1, -4]$. Thus, the eigenvalues of \mathbf{A} are equal to $[1 - \cos(2\pi k/N)]^2$. Hence,

application of Eq. (16) yields

$$\sigma_{\text{lin}}^2(t) = \frac{1}{g_c} \int_0^{g_c t} \frac{2}{N} \sum_{k=0}^{N-1} \left[1 - \cos\left(\frac{2\pi k}{N}\right) \right] \times e^{-8\tau' [1 - \cos(2\pi k/N)]^2} d\tau'. \quad (\text{B3})$$

Taking the limit of the last formula as $N \rightarrow \infty$, we find

$$\sigma_{\text{lin}}^2(t) = \frac{2}{g_c} \int_0^{g_c t} \int_0^1 [1 - \cos(2\pi z)] e^{-8\tau' [1 - \cos(2\pi z)]^2} dz d\tau'. \quad (\text{B4})$$

Evidently, for finite t , the variance is bounded; more precisely, $\sigma_{\text{lin}}^2(t) \leq 4t$.

To evaluate $\sigma_{\text{lin}}^2(t)$ for $g_c t \gg 1$, we fix some intermediate time $t_0 = \mathcal{O}(1)$ and rewrite Eq. (B4) as

$$\sigma_{\text{lin}}^2(t) = \sigma_{\text{lin}}^2(t_0) + \frac{2}{g_c} \int_{g_c t_0}^{g_c t} \int_0^1 [1 - \cos(2\pi z)] \times e^{-8\tau' [1 - \cos(2\pi z)]^2} dz d\tau', \quad (\text{B5})$$

where $\sigma_{\text{lin}}(t_0) = \mathcal{O}(1)$. The second term on the right-hand side of Eq. (B5) can be approximated asymptotically with ease, since $\tau' \geq g_c t_0 \gg 1$. By the identity $1 - \cos(2\pi z) = 2\sin^2(\pi z)$, symmetry of the integrand about $z = 1/2$ and the change of variable $x = \sin(\pi z)$, Eq. (B5) is recast to

$$\begin{aligned} \sigma_{\text{lin}}^2(t) &\sim \sigma_{\text{lin}}(t_0)^2 + \frac{8}{\pi g_c} \int_{g_c t_0}^{g_c t} \int_0^\infty \frac{x^2}{\sqrt{1-x^2}} e^{-32\tau' x^4} dx d\tau' \\ &\sim \sigma_{\text{lin}}(t_0)^2 + \frac{8}{\pi g_c} \int_{g_c t_0}^{g_c t} \int_0^\infty x^2 e^{-32\tau' x^4} dx d\tau' \end{aligned} \quad (\text{B6})$$

where we used $(1-x^2)^{-1/2} = 1 + o(1)$ in the integrand, since for fixed $\tau' \gg 1$ the major contribution to integration in x arises from $x = 0$. In Eq. (B6), the inner integral may be computed exactly to yield [40]

$$\sigma_{\text{lin}}^2(t) \sim \sigma(t_0)^2 + g_c^{-1} \int_{g_c t_0}^{g_c t} \frac{\Gamma(3/4)}{4\pi(2\tau')^{3/4}} d\tau'. \quad (\text{B7})$$

Further integration furnishes the anticipated behavior $\sigma_{\text{lin}}^2(t) = \mathcal{O}[(g_c t)^{1/4}]$ as $g_c t \rightarrow \infty$.

2. MF approximation

In this subsection, we derive Eq. (41), the leading-order variance for the steady-state TWD, $P_0(s)$. By Eq. (39), we write the MF variance from Eq. (40) as

$$\begin{aligned} \sigma_0^2 &= \mathcal{N}_0 \int_0^\infty (y-1)^2 \\ &\times \exp\left\{ \frac{g}{3} \int_1^y \left[\frac{4}{\xi+c} + \frac{2}{c+1} \right] \left[\frac{1}{\xi^3} - 1 \right] d\xi \right\} dy \\ &= \mathcal{N}_0 \int_0^\infty (y-1)^2 \exp\left(\frac{g}{3} \int_1^y A(\xi, 1) d\xi \right) dy. \end{aligned} \quad (\text{B8})$$

Next, we compute integral (B8) by a change of variable. So, define the mapping $y \mapsto v$ where

$$v(y) = \frac{g}{3} \int_1^y A(\xi, 1) d\xi, \quad (\text{B9})$$

$$\begin{aligned} v(y) &\rightarrow 0 \quad \text{as } y \rightarrow 1, \text{ and} \\ v(y) &\rightarrow -\infty \quad \text{as } y \rightarrow 0 \text{ or } y \rightarrow \infty. \end{aligned}$$

Note that $y(v)$ is a double-valued function of v . To render $y(v)$ single valued, one must restrict y in $(0, 1)$ or $(1, \infty)$ (i.e., on the left or right of the maximum of $P_0(s)$, as suggested by Fig. 2). Hence, we write Eq. (B8) as

$$\begin{aligned} \sigma_0^2 &= \mathcal{N}_0 \int_0^1 (y-1)^2 e^{v-(y)} dy \\ &\quad + \mathcal{N}_0 \int_1^\infty (y-1)^2 e^{v+(y)} dy \\ &= \frac{3}{g} \mathcal{N}_0 \left\{ \int_{-\infty}^0 [y(v_-) - 1]^2 \frac{e^{v_-}}{A(y(v_-), 1)} dv_- \right. \\ &\quad \left. - \int_{-\infty}^0 [y(v_+) - 1]^2 \frac{e^{v_+}}{A(y(v_+), 1)} dv_+ \right\}, \end{aligned} \quad (\text{B10})$$

where $v_{\pm(-)}$ represents values of v if $y > 1$ ($0 < y < 1$). Regarding the normalization constant \mathcal{N}_0 , we note that

$$\begin{aligned} \mathcal{N}_0 &\left[\int_0^1 e^{v-(y)} dy + \int_1^\infty e^{v+(y)} dy \right] \\ &= \frac{3\mathcal{N}_0}{g} \left[\int_{-\infty}^0 \frac{e^{v-(y)}}{A(v_-, 1)} dv_- - \int_{-\infty}^0 \frac{e^{v+(y)}}{A(v_+, 1)} dv_+ \right] \\ &= 1. \end{aligned} \quad (\text{B11})$$

The task is to compute \mathcal{N}_0 and thereby σ_0^2 . Since $dy = 3 dv_{\pm} / \beta A(y(v_{\pm}), 1)$, the transformed integrand as a function of v_{\pm} exhibits a singularity as $v_{\pm} \rightarrow 0$.

We first derive an explicit expression for y as a function of v_{\pm} . By the definition of $v(y)$, Eq. (B9), for large g we expect that the major contribution to integration in Eq. (B11) stems from a neighborhood of $v_{\pm} = 0$, or $y = 1$. Hence, by Taylor expanding the right-hand side of Eq. (B9) around $y = 1$ we have

$$y-1 = \pm \sqrt{\frac{-(c+1)v_{\pm}}{3\beta}} + \mathcal{O}(\beta^{-1}), \quad (\text{B12})$$

as $v_{\pm} \rightarrow 0$. So, we obtain the simplified expression

$$\begin{aligned} \frac{gA(y(v_{\pm}), 1)}{3} &\sim \frac{g}{3} \left[\frac{4}{c+1 \pm \sqrt{\frac{-(c+1)v_{\pm}}{3\beta}}} + \frac{2}{c+1} \right] \\ &\quad \times \left[\left(1 + \sqrt{\frac{-(c+1)v_{\pm}}{3\beta}} \right)^{-3} - 1 \right] \\ &\sim \pm 2 \sqrt{\frac{-3gv_{\pm}}{c+1}} \quad \text{as } v_{\pm} \rightarrow 0. \end{aligned} \quad (\text{B13})$$

Thus, to leading order in g , we assert that

$$1 = \int_0^\infty P_0(y) dy \sim \mathcal{N}_0 \int_{-\infty}^0 \sqrt{\frac{c+1}{-3gv}} e^v dv, \quad (\text{B14})$$

which in turn implies

$$\mathcal{N}_0 = \mathcal{N}_0(g, c) \sim \sqrt{\frac{3g}{\pi(c+1)}}. \quad (\text{B15})$$

The substitution of Eqs. (B12), (B13), and (B15) into Eq. (B10) yields formula (41).

Appendix C: Kinetic Monte Carlo simulation

In this appendix, we provide some details on our 1D kMC method. This algorithm follows the general methods set forth in Refs. [17, 41, 42]. We consider a system of descending steps (Fig. 1), which are viewed as particles at positions x_j on a lattice with spacing Δx in 1D. We apply screw periodic boundary conditions, so that when a step moves off from one end, another step re-enters from the other end. The particles are only allowed to move to lattice sites, and overlaps and crossings are prohibited.

We proceed to prescribe the particle kinetics. The j th step is assigned two energy barriers, $E_j(\pm\Delta x)$: one for the step to move right (+) and another barrier for the step to move left (-). Each of these barriers forms a linear combination of four repulsive energies, each proportional to the inverse distance squared between a given step and one of its four nearest neighbors, i.e.,

$$E_j(\pm\Delta x) = \sum_{\substack{k=j-2 \\ k \neq 0}}^{j+2} \frac{b}{|x_j \pm \Delta x - x_{j+k}|^2} - \frac{b}{|x_j - x_{j+k}|^2}, \quad (\text{C1})$$

where b is an adjustable parameter with units of energy. By Eq. (C1), if a step is one lattice site (distance Δx) away from one of its nearest neighbors, the energy barrier for closer approach becomes infinite, prohibiting movement. Thus, for each of the two directions that a step is allowed to move to, we define the transition rate

$$R_j(\pm\Delta x) = \exp\left(\frac{-E_j(\pm\Delta x)}{k_B T}\right). \quad (\text{C2})$$

This definition comes from standard transition state theory [17, 42]. The underlying concept is that a particle in a statistical ensemble at temperature T will be excited to the energy of the barrier with probability given by the usual Arrhenius formula. It is assumed that, having reached the peak of the barrier, the step makes a transition to the neighboring state with probability one.

We subsequently define two ‘‘movement classes’’ for right- and left-moving particles (steps). The corresponding total rate is taken to be

$$R_{\text{tot}}^\pm = \sum_j R_j(\pm\Delta x). \quad (\text{C3})$$

Transitions requiring infinite energy do not contribute to this sum. After division by $R_{\text{tot}}^+ + R_{\text{tot}}^-$, Eq. (C3) yields the probability that *some* step moves either left or right.

Three random numbers between 0 and 1 are generated and used in the following way. The first number determines from which movement class to select a particle to move according to the relative ratios of the two total class rates. The second random number picks the particle within the movement class that will move. Lastly, the third number, say r_3 , determines for how long (in simulation time) the transition occurs according to the relation $\Delta t = -\omega_{\text{vib}} \ln(r_3)$, where ω_{vib} characterizes how often the step attempts to leave its lattice site. The constant ω_{vib} is kept at a fixed value (equal to 10 in our simulations), since the time scaling of the simulation can be chosen at will.

After performing these tasks, we update the position of each step and iterate the procedure for a specified number of times. For the b entering Eq. (C1) we use values ranging from 1×10^0 to 2×10^6 . These high numbers might seem puzzling. However, our 1D model does *not* follow adatoms but steps. For the sake of comparisons with our analytical results, we fix the number of steps at 50, with a uniform, initial spacing of 100 lattice units (length $100\Delta x$). The large initial step spacing is due to the need to have fine scale resolution of the kMC TWD peak in order to compare it with the analytically derived TWD.

To reach the steady state, we run simulations of 5×10^4 and 10^5 iterations; we average over $(1-2) \times 10^4$ runs. A characteristic feature of these runs with $0 < b \leq \mathcal{O}(10^2)$ is a *tendency* exhibited by the TWD to approach a Poisson distribution for long times, with the TWD peak moving nearly to zero terrace width. The singular interaction, however, always prevents the steps from touching or crossing, and hence the TWD goes sharply to zero for zero terrace width. With increasing interactions, the peak tends not to move as far left (close to the origin), and the system equilibrates much more quickly.

Fitting the analytic TWD’s (20), (40), or (43) to the kMC TWD requires the determination of both the parameters c and g . Recall that g is a measure of the interaction strength, while c is a length expressing the interplay between diffusion and attachment-detachment processes of *adatoms*. We cannot estimate a priori what value of c corresponds to our kMC simulation because the algorithm follows steps and not adatoms.

Since the peak of the kMC TWD moves left of the initial width for all values of b studied, neither of the analytic expressions (20) or (40) provides a good fit to the kMC TWD except when $b = \mathcal{O}(10^6)$ (when all of the analytic TWD’s approach a Gaussian distribution). Hence, the composite TWD (43) is used in all cases to determine c and g . We find that for any *fixed* $c \geq \mathcal{O}(10)$, g may be used as the sole fitting parameter, and that for fixed b , changing the value of c ($c \geq \mathcal{O}(10)$) does not noticeably change the fit, provided the ratio g/c is constant. This last observation is justified by examination

of Eqs. (42) and (43); when $c \geq \mathcal{O}(10)$, the correction to the mean field f_1/g scales approximately as $c/3g$, and $gA(s, f) \approx (6g/c)(s^{-3} - f^{-3}(s))$. In the end, for our kMC simulation we have $1650 \leq g \leq 8400$.

For values of $c < \mathcal{O}(10)$, the peak of the analytic solu-

tion is to the left of the kMC TWD peak, and no value of g provides a good fit. Hence, our kMC simulation corresponds to a system in which attachment-detachment limited kinetics are the dominant mass transport mechanisms.

-
- [1] Th. Seyller, A. Bostwick, K. M. Emtsev, K. Horn, L. Ley, J. L. McChesney, T. Ohta, J. D. Riley, E. Rotenberg, and F. Speck, *Physica Status Solidi* **245**, 1436 (2008).
- [2] A. Kühnle, *Current Opinion Coll. Interface Sci.* **14**, 157 (2009).
- [3] H.-C. Jeong and E. D. Williams, *Surf. Sci. Rep.* **34**, 171 (1999).
- [4] O. Pierre-Louis and C. Misbah, *Phys. Rev. B* **58**, 2259 (1998).
- [5] T. Ihle, C. Misbah, and O. Pierre-Louis, *Phys. Rev. B* **58**, 2289 (1998).
- [6] A. Pimpinelli, H. Gebremariam, and T. L. Einstein, *Phys. Rev. Lett.* **95**, 246101 (2005).
- [7] A. BH. Hamouda, A. Pimpinelli, and T. L. Einstein, *Europhys. Lett.* **88**, 26005 (2009).
- [8] P. Nozières, in *Solids Far from Equilibrium*, edited by C. Godrèche (Cambridge University Press, Cambridge, UK, 1991).
- [9] R. Balescu, *Equilibrium and Non-equilibrium Statistical Mechanics*, Wiley, New York, 1975.
- [10] D. Margetis, *J. Phys. A: Math. Theor.* **43**, 065003 (2010).
- [11] W. K. Burton, N. Cabrera, and F. C. Frank, *Phil. Trans. R. Soc. London A* **243**, 299 (1951).
- [12] E. E. Gruber and W. W. Mullins, *J. Phys. Chem. Solids* **28**, 875 (1967).
- [13] V. I. Marchenko and A. Ya. Parshin, *Soviet Phys. JETP* **52**, 129 (1980).
- [14] R. Najafabadi and D. J. Srolovitz, *Surf. Sci.* **317**, 221 (1994).
- [15] Z. Schuss, *Theory and Applications of Stochastic Processes: An Analytical Approach* (Springer, New York, 2010).
- [16] M. Uwaha and Y. Saito, *Phys. Rev. Lett.* **68**, 224 (1992).
- [17] J. G. Amar, *Computing Sci. Eng.* **8**, 9 (2006).
- [18] R. Ghez and S. S. Iyer, *IBM J. Res. Develop.* **32**, 804 (1988).
- [19] R. Ghez, H. G. Cohen, and J. B. Keller, *J. Appl. Phys.* **73**, 3685 (1993).
- [20] M. Ozdemir and A. Zangwill, *Phys. Rev. B* **42**, 5013 (1990).
- [21] G. S. Bales and A. Zangwill, *Phys. Rev. B* **41**, 5500 (1990).
- [22] F. Liu and H. Metiu, *Phys. Rev. E* **49**, 2601 (1997).
- [23] J. Krug, in *Nonlinear Dynamics of Nanosystems*, edited by G. Radons, B. Rumpf, and H. G. Schuster (Wiley-VCH, Weinheim, 2010).
- [24] P. Nozières, *J. Phys. (France)* **48**, 1605 (1987).
- [25] G. Ehrlich and F. Hudda, *J. Chem. Phys.* **44**, 1039 (1966).
- [26] R. L. Schwoebel and E. J. Shipsey, *J. Appl. Phys.* **37**, 3682 (1966).
- [27] By elementary probability theory (i.e., use of the Chebyshev inequality), the probability for step crossing is controlled by the terrace width variance.
- [28] Specifying the precise conditions needed to define a consistent noise term is an open problem.
- [29] H. Risken, *The Fokker-Planck Equation: Methods of Solution and Applications*, 2nd ed. (Springer, Berlin, 1989).
- [30] C. M. Bender and S. Orszag, *Advanced Mathematical Methods for Scientists and Engineers* (Springer, New York, 1999).
- [31] The subscript s in P_s here indicates the steady state and should not be confused with the partial derivative in s .
- [32] Bateman Manuscript Project, *Higher Transcendental Functions, Vol. II*, edited by A. Erdélyi et al. (Krieger, Malabar, FL, 1981).
- [33] Dominant balance essentially amounts to matching the exponents of the expansion parameter g . For details see Ref. 30.
- [34] D. R. M. Williams and M. Krishnamurthy, *Appl. Phys. Lett.* **62**, 1350 (1993).
- [35] S. Tanaka, N. C. Bartelt, C. C. Umbach, R. M. Tromp, and J. M. Blakely, *Phys. Rev. Lett.* **78**, 3342 (1997); S. Stoyanov and V. Tonchev, *Phys. Rev. B* **58**, 1590 (1998); W. F. Chung, K. Bromann, and M. S. Altman, *Int. J. Mod. Phys. B* **16**, 4353 (2002).
- [36] E.S. Fu, M.D. Johnson, D.-J. Liu, J.D. Weeks, E.D. Williams, *Phys. Rev. Lett* **77** (1996) 1091.
- [37] U. Grenander and G. Szegő, *Toeplitz Forms and Their Applications* (University of California Press, Berkeley, CA, 1958).
- [38] Nicholas J. Higham, *Functions of Matrices: Theory and Computation* (SIAM, Philadelphia, 2008).
- [39] In the case that one or more of the eigenvalues ϑ_k are 0, it is sufficient to add and subtract $\hat{\theta}\mathbf{1}$, $\hat{\theta} > \max_k |\vartheta_k|$ to $\mathbf{X}\mathbf{X}^T$ and separate the resulting term into two matrices with non-zero eigenvalues. By linearity of the trace operator the result then holds.
- [40] Bateman Manuscript Project, *Higher Transcendental Functions, Vol. I*, edited by A. Erdélyi et al. (Krieger, Malabar, FL, 1981).
- [41] A. F. Voter, in *Radiation Effects in Solids*, edited by K. E. Sickafus, E. A. Kotomin, and B. P. Uberuaga (Springer, NATO Science Series, Dordrecht, 2007).
- [42] T. Ala-Nissila, R. Ferrando, and S. C. Ying, *Adv. Phys.* **51**, 949 (2002).